AD_____

Award Number: W81XWH-11-1-0669

TITLE: Role of p53 in cdk Inhibitor VMY-1-103-Induced Apoptosis in Prostate Cancer

PRINCIPAL INVESTIGATOR: Lymor Ringer

CONTRACTING ORGANIZATION: Georgetown University, Washington, DC 20057

REPORT DATE: September 2012

TYPE OF REPORT: Annual Summary

PREPARED FOR: U.S. Army Medical Research and Materiel Command
Fort Detrick, Maryland 21702-5012

# REPORT DOCUMENTATION PAGE

*Form Approved*
*OMB No. 0704-0188*



| 1. REPORT DATE | 2. REPORT TYPE | 3. DATES COVERED |
|---|---|---|
| 01-09-2012 | Annual Summary | 22 Aug 2011 - 21 Aug 2012 |

**4. TITLE AND SUBTITLE**
Role of p53 in cdk inhibitor VMY-1-103-induced apoptosis in Prostate cancer

**5a. CONTRACT NUMBER**

**5b. GRANT NUMBER**
W81XWH-11-1-0669

**5c. PROGRAM ELEMENT NUMBER**

**6. AUTHOR(S)**
Lymor Ringer

E-Mail: LRR28@georgetown.edu

**5d. PROJECT NUMBER**

**5e. TASK NUMBER**

**5f. WORK UNIT NUMBER**

**7. PERFORMING ORGANIZATION NAME(S) AND ADDRESS(ES)**
Georgetown University, Washington, DC 20057

**8. PERFORMING ORGANIZATION REPORT NUMBER**

**9. SPONSORING / MONITORING AGENCY NAME(S) AND ADDRESS(ES)**
U.S. Army Medical Research and Materiel Command
Fort Detrick, Maryland 21702-5012

**10. SPONSOR/MONITOR'S ACRONYM(S)**

**11. SPONSOR/MONITOR'S REPORT NUMBER(S)**

**12. DISTRIBUTION / AVAILABILITY STATEMENT**
Approved for Public Release; Distribution Unlimited

**13. SUPPLEMENTARY NOTES**

**14. ABSTRACT**

Cyclin-dependent kinase inhibitor VMY-1-103 induces a G2/M cell cycle arrest and apoptosis in prostate cancer cell lines. Cancer cell lines, including prostate cancer, show a differential sensitivity to VMY-1-103 that correlates with p53 status. In addition, VMY-1-103 sensitivity increases in cancer cell lines as compared with normal cell lines, regardless of p53 status. Knockdown experiments in LNCaP cells show a reduced sensitivity to VMY-1-103 by resulting in a decreased cell death and this result can be rescued by the addition of wild-type p53. Transient transfections of wild-type p53 into p53-null PC-3 cells resulted in increased cell death upon VMY treatment. Furthermore, PRIMA-1 pre-treatment restored p53 activity in p53-mutant DU145 cells and sensitized them to VMY-mediated cell death. As compared with other solid tumors, only a small percentage of prostate cancer cases contain p53 mutations. Therapeutically, this is important as a majority of prostate cancer patients could benefit from VMY.

**15. SUBJECT TERMS**
P53, apoptosis, cyclin-dependent kinase inhibitor

| 16. SECURITY CLASSIFICATION OF: | | | 17. LIMITATION OF ABSTRACT | 18. NUMBER OF PAGES | 19a. NAME OF RESPONSIBLE PERSON |
|---|---|---|---|---|---|
| a. REPORT | b. ABSTRACT | c. THIS PAGE | | | USAMRMC |
| U | U | U | UU | 26 | 19b. TELEPHONE NUMBER *(include area code)* |

## Table of Contents

Introduction:

The mammalian cell cycle is a tightly regulated process that controls cell division and replication. The tumor suppressor p53 plays a crucial role in both the G1/S and mitotic checkpoints, as well as in apoptosis in response to DNA damage. P53 activates p21, which is an inhibitor of cdk/cyclin E complexes, to cause cell cycle arrest. P53 can also function as a mediator of apoptosis by activating either the intrinsic or extrinsic pathway of apoptosis via transcriptional targets such as Bax, Bid, and TRAIL R4/5 (1). Deregulation of the cell cycle has been described in many human tumors, including prostate cancer (2). In prostate cancer specifically, cyclinD1 has been shown to be upregulated while down-regulation is commonly seen in cyclin-dependent kinase (cdk) inhibitors such as $p16^{INK4A}$ and $p27^{Kip1}$ (3). Therefore, small molecule cyclin dependent kinase (cdk) inhibitors may have the ability to block tumor progression in prostate cancer. We have developed a novel analog of purvalanol B termed VMY-1-103 (VMY) that functions as a potent cdk1 and cdk2 inhibitor. VMY shows enormous potential as a therapeutic agent for prostate cancer treatment.

Body:

Aim 1 is to test VMY-1-103 on a panel of human prostate cancer cell lines and correlate activity with p53 status. VMY-1-103 was tested on a large panel of cancer and normal cell lines. These cell lines include prostate cancer cell line LNCaP, which is p53 wild-type, PC3 cells, which are null, and DU145 cells that contain p53 mutations. VMY-1-103 sufficiently caused an increase in cells in G2/M and greater than 40% cell death in LNCaP cells ($p<0.05$) as measured by trypan blue exclusion in 18 hours. In contrast the parent compound, purvalanol B, was only able to cause 2% cell death in these cells. Furthermore, less than 5% cell death was seen upon treatment of the PC3 and DU145 cells, although a G2/M arrest was seen in both cell types. Cell death in LNCaP cells was confirmed as apoptosis by an apoptosis protein expression array. Results showed that VMY treatment led to a significant increase in PARP cleavage and cleaved caspase 3, which are clear markers of apoptosis. In addition, VMY treatment led to an increase in phosphorylated levels of p53 (S15, S46, and S392) as well as total p21 levels, suggesting p53 is important in the apoptotic response following VMY treatment (4). Interestingly, VMY is able to induce a cell cycle arrest at the G2/M checkpoint in all cells, but the apoptotic factor seems to be related to p53 status.

Additional wild-type p53 cancer cell lines, PC12, A172, MCF7, and COLO-357, were all sensitive to VMY-1-103 treatment at similar rates as LNCaPs. In addition, other p53 mutant cell lines ASPC1, MIA-PaCa1, MDA231, and T98G, had less than 5% cell death following treatment. Furthermore, four additional prostate cell lines were generated from two patients; two normal cell lines (029N and 003N) and two tumor lines (030T and 004T). These cells were generated using methods developed at Georgetown University and all of these cell lines are p53 wild-type (5). Interestingly, the tumor cell line is more sensitive to cell death with VMY treatment than the normal cells (figure 1).

Our research has shown that VMY can cause chromosomal abnormalities and induce mitotic catastrophe in DAOY medulloblastoma cells, which have a p53 mutation (6). In order to examine if this holds true in prostate cancer cell lines, I stably transfected LNCaP and DU145

cells with a GFP HistoneH2B construct. I then performed time-course live cell imaging as previously described (6). In contrast to what was observed with the DAOY cells, no mitotic castrophe or delay of mitosis was seen. In addition, I performed confocal microscopy on LNCaP and DU145 cells stained with Aurora A and did not observe any mitotic abnormalities. Due to these results, I did not continue exploring the effects of VMY on these cells and did not do live imaging of the p53 knockdown or overexpressed cells as proposed as Aim 2d.

Aim 2 is to determine if wild-type p53 is required for VMY-1-103-induced apoptosis. To test this, I first performed siRNA knockdown of p53 in wild-type LNCaP cells (figure 2a). Briefly, cells were incubated with either adenovirus alone or adenovirus containing p53 siRNA. I next treated these knockdown cells with VMY and found that reduction in wild type levels of p53 greatly reduced the ability of VMY to cause cell death in these cells (figure 2b). In addition, I performed an apoptosis protein expression array on the p53 knockdown cells with and without VMY treatment and found that apoptosis was greatly reduced in the knockdown cells following VMY treatment as measured by Bax, cleaved Caspase 3, and TRAIL DR5 (figure 2d). Furthermore, I performed an siRNA rescue experiment in which I knocked down p53, transfected with a WT expression vector, and then treated cells with VMY. Ability to cause cell death was rescued as seen by an increase in cell death (figure 2c).

I next overexpressed WT p53 in PC3 (null) cells, which greatly sensitized them to VMY-induced cell death. I also transiently transfected mutant p53 (245), which did not affect cell death upon VMY treatment as compared with GFP transfection alone (figure 3). Because DU145 cells inherently have two p53 mutations with unknown functions, I could not simply overexpress a wild-type vector in these cells. Instead, I pre-treated these cells with a drug called PRIMA-1, which can restore wild-type function of p53 in cells with mutations in the DNA binding domain, such as DU145 (7). Upon treatment with PRIMA-1, p21 levels are restored in DU145, suggesting restoration of p53 function (figure 4a). Following PRIMA-1 pretreatment, I treated cells with flavopiridol, purvalanol B, or VMY and found that there was an increased sensitivity to cell death (figure 4b), although no changes in the cell cycle distribution as measured by flow cytometry. Furthermore, PRIMA-1 pre-treatment led to an increase in PARP cleavage upon VMY treatment, confirming an increase in apoptosis upon restoration of WT p53 (figure 4c).

Because I determined that WT p53 plays an important role in causing cell death upon VMY treatment in these cells, I next tested if mutant p53 constructs had the same effect. I created stable tet-on inducible LNCaP cells overexpressing mutant p53 at hotspot mutation sites 245 and 175 (Figure 5a). Upon VMY treatment, the overexpression of a mutant p53 construct did not change the cell cycle profile or ability of VMY to cause cell death. Because wild-type p53 is still present in these cells, I next knocked down wt p53 using siRNA, and then induced the mutant constructs using tetracycline. The knockdown of p53 alone inhibited the effect of VMY on halting the cell cycle and this effect was not rescued by the induction of either mutant construct (Figure 5b).

Aim 3 is to test VMY-1-103 in prostate cancer xenograph mouse models and this work is currently ongoing. In addition, a manuscript for AIM 2 is being written and there are plans for paper submission within the next few months.

Key Research Accomplishments:

- Expanded testing of VMY-1-103 to many cancer and normal cell lines.
- Strengthened correlation between efficacy of VMY-1-103 to cause apoptosis and p53 status in cell lines.
- Showed that knockdown of p53 in wild-type LNCaP cells greatly reduces sensitivity to VMY. This effect can also be rescued by addition of a wild-type p53 vector following siRNA knockdown. Mutant p53 constructs did not rescue this effect.
- Further confirmed that wild type p53 is required for VMY-mediated apoptosis by restoring wild type p53 function in p53 mutant DU145 cells, which greatly increased their sensitivity to the drug. Furthermore, transient transfection of wild-type p53 in p53 null PC3 cells rendered them sensitive to VMY.

Reportable Outcomes:

- First author publication:
  - **Ringer L**, Sirajuddin P, Heckler M, Ghosh A, Suprynowicz F, Yenugonda VM, Brown ML, Toretsky JA, Uren A, Lee Y, Macdonald TJ, Rodriguez O, Glazer RI, Schlegel R, Albanese C. VMY-1-103 is a novel CDK inhibitor that disrupts chromosome organization and delays metaphase progression in medulloblastoma cells. **Cancer Biol Ther**. 2011 Nov 1;12(9):818-26
- Other publications:
  - Beauchamp EM, **Ringer L**, Bulut G, Sajwan KP, Hall MD, Lee YC, Peaceman D, Ozdemirli M, Rodriguez O, Macdonald TJ, Albanese C, Toretsky JA, Uren A. Arsenic trioxide inhibits human cancer cell growth and tumor development in mice by blocking Hedgehog/GLI pathway. **J Clin Invest**. 2011 Jan 4;121(1):148-60
- Poster Presentations:
  - American Association for Cancer Research Annual Meeting, Chicago IL. Role of p53 in CDK Inhibitor VMY-1-103-mediated Apoptosis . March 31$^{st}$ – April 4$^{th}$, 2012.
  - Georgetown University Student Research Day. Role of p53 in CDK Inhibitor VMY-1-103-mediated Apoptosis. March 1$^{st}$, 2012 Washington, DC.
  - Georgetown University Student Research Day. CDK Inhibitor VMY-1-103 Causes Cell Cycle Arrest and Apoptosis in Cancer Cell Lines. April 7$^{th}$, 2011 Washington, DC.
  - Cell cycle Regulators/Inhibitors & Cancer. CDK Inhibitor VMY-1-103 Causes Cell Cycle Arrest and Apoptosis in Cancer Cell Lines. February 5$^{th}$-8$^{th}$, 2011 Vienna, Austria.

Conclusion:

Cyclin-dependent kinase inhibitor VMY-1-103 induces a G2/M cell cycle arrest and apoptosis in prostate cancer cell lines. Cancer cell lines, including prostate cancer, show a differential sensitivity to VMY-1-103 that correlates with p53 status. In addition, VMY-1-103 sensitivity increases in cancer cell lines as compared with normal cell lines, regardless of p53 status. This has important therapeutic implications for the treatment of prostate cancer patients. Knockdown experiments in LNCaP cells show a reduced sensitivity to VMY-1-103 by resulting in a decreased cell death and this result can be rescued by the addition of wild-type p53. Transient transfections of wild-type p53 into p53-null PC-3 cells resulted in increased cell death upon VMY treatment. Furthermore, PRIMA-1 pre-treatment restored p53 activity in p53-mutant DU145 cells and sensitized them to VMY-mediated cell death. As compared with other solid tumors, only a small percentage of prostate cancer cases contain p53 mutations (8). Therapeutically, this is important as a majority of prostate cancer patients could benefit from VMY treatment. Furthermore, p53 mutations are generally only seen in prostate cancer patients who have very aggressive tumors. Therefore, VMY may be a more useful therapeutic to use to treat earlier stages of prostate cancer than aggressive, metastatic cancer. Further studies are ongoing to test VMY in aggressive tumors, either by modulating the p53 status in the tumors or by combining VMY with other therapeutic agents.

References:


1) Chakravarti A, Heydon K, Wu CL, et al. Loss of p16 expression is of prognostic significance in locally advanced prostate cancer: an analysis from the radiation therapy oncology group protocol 86-10. J Clin Oncol. 2003; 21: 3328-3334.

2) Casimiro M, Rodriguez O, Pootrakul L, Aventian M, Lushina N, Cromelin C, et al. ErbB-2 induces the cyclin D1 gene in prostate epithelial cells in vitro and in vivo. Cancer Res 2007; 67:4364-72.

3) Shapiro, G.I. Cyclin-dependent kinase pathways as targets for cancer treatment. J Clin Oncol. 2006: 24: 1770-1783.

4) Ringer L, Sirajuddin P, Yenugonda VM, Ghosh A, Divito K, Trabosh V, Patel Y, Brophy A, Avantaggiati ML, Grindrod S, Lisani M, Rosenthal D, Brown ML, Rodriguez OC, Albanese C. VMY-1-103, a dansylated analog of purvalanol B, induces caspase-3 - dependent apoptosis in LNCaP prostate cancer cells. Cancer Biol Ther. 2010 Aug;10(4):320-5.

5) Liu X, Ory V, Chapman S, Yuan H, Albanese C, Kallakury B, Timofeeva OA, Nealon C, Dakic A, Simic V, Haddad BR, Rhim JS, Dritschilo A, Riegel A, McBride A, Schlegel R. ROCK inhibitor and feeder cells induce the conditional reprogramming of epithelial cells. Am J Pathol. 2012 Feb;180(2):599-607.

6) Ringer L, Sirajuddin P, Heckler M, Ghosh A, Suprynowicz F, Yenugonda VM, Brown ML, Toretsky JA, Uren A, Lee Y, MacDonald TJ, Rodriguez O, Glazer RI, Schlegel R, Albanese C. VMY-1-103 is a novel CDK inhibitor that disrupts chromosome organization and delays metaphase progression in medulloblastoma cells. Cancer Biol Ther. 2011 Nov 1;12(9):818-26.

7) Lambert JM, Gorzov P, Veprintsev DB, Söderqvist M, Segerbäck D, Bergman J, Fersht AR, Hainaut P, Wiman KG, Bykov VJ. PRIMA-1 reactivates mutant p53 by covalent binding to the core domain. Cancer Cell. 2009 May 5;15(5):376-88.

8) Dong JT. Prevalent mutations in prostate cancer. J Cell Biochem. 2006 Feb 15;97(3):433-47.

Supporting Data:

*Figure 1*: VMY-1-103 causes a larger amount of cell death in primary tumor cells compared with normal adjacent cells.

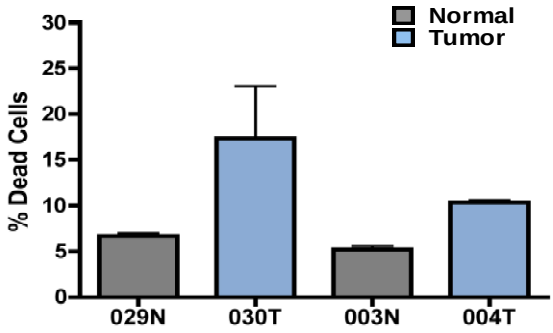


*Figure 1*: Percentage of cell death following 18hr of VMY treatment as quantified by trypan blue dye exclusion. 029N (normal) and 030T (tumor) are one patient and 003N (normal) and 004T (tumor) are from another patient. Cell death significantly increases in tumor cells as compared with the matched sets of normal cells.

*Figure 2*: Knockdown of p53 in LNCaP cells greatly reduces VMY-1-103-mediated apoptosis

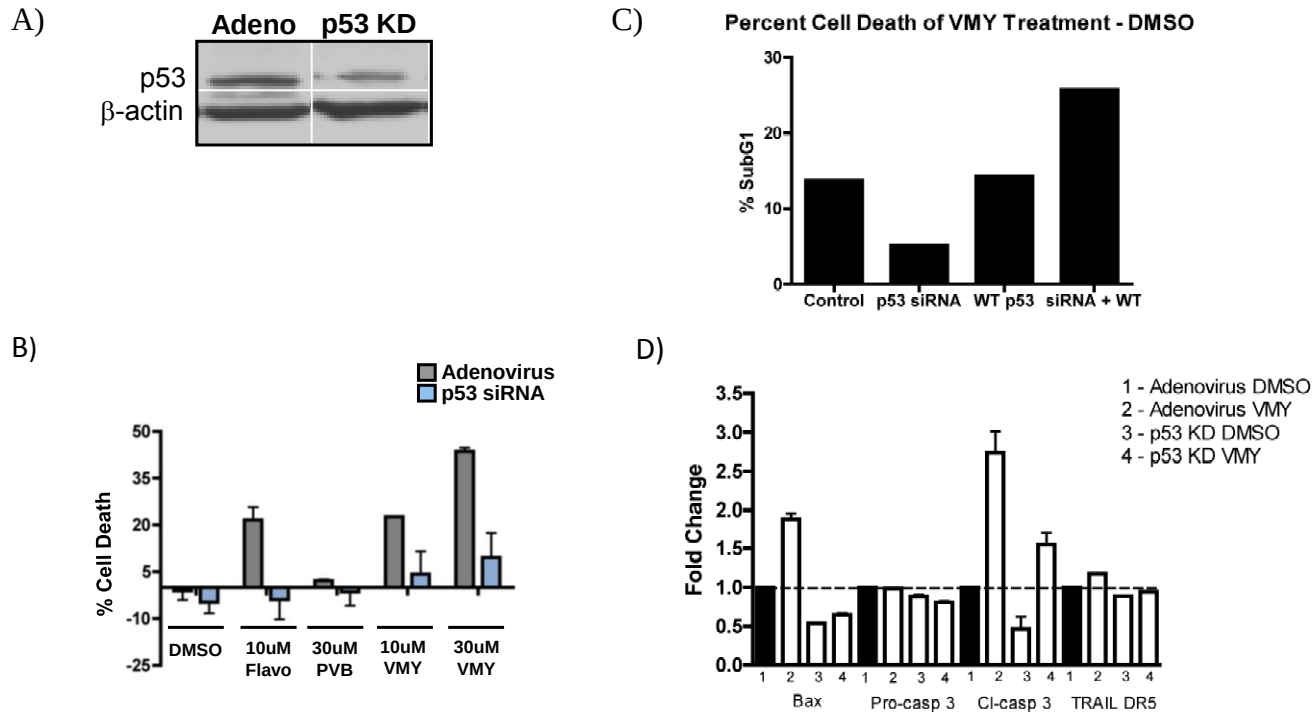


*Figure 2*: A) P53 protein levels in LNCaP cells decrease after addition of a p53 siRNA adenovirus for 72hr as compared to addition of adenovirus alone. B) LNCaP cells were treated with either adenovirus or p53 siRNA for 72hrs, followed by treatment with either flavopiridol (Flavo), purvalanol B (PVB), 10uM or 30uM VMY for 18hr. Cell death was quantified by trypan blue dye exclusion. C) LNCaP cells with and without p53 siRNA were transfected with a wild-type p53 vector, followed by treatment with either DMSO or VMY. Percentage of cell death was quantified by the subG1 fraction of cells using flow cytometry. The percentage of dead cells with DMSO treatment was subtracted from the percentage of dead cells after VMY treatment. D) VMY-1-103 treatment in the presence of adenovirus alone induce apoptosis as measured by an increase in Bax, cleaved Caspase 3, and TRAIL DR5 protein levels. These levels are reduced following p53 siRNA treatment.

*Figure 3*: Addition of wild-type p53 into p53 null PC3 cells greatly sensitizes them to VMY treatment.

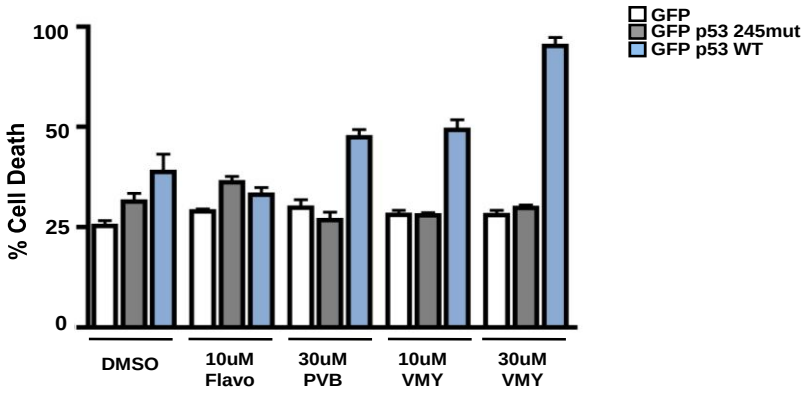


*Figure 3*: Transient transfection of either GFP, GFP-mutant 245 p53, or GFP-WT p53 constructs in PC3 cells followed by treatment with either DMSO, flavopiridol, purvalanol B (PVB), 10uM, or 30uM VMY. Percentage of cell death was measured by subG1 quantification using flow cytometry. Mutant p53 in addition to any drug treatment did not affect cell death, while WT p53 greatly increased cell death following purvalanol B and VMY treatment.

*Figure 4*: Treatment of p53-mutant DU145 cells with PRIMA-1 restores wild-type p53 function and sensitizes the cells to VMY.

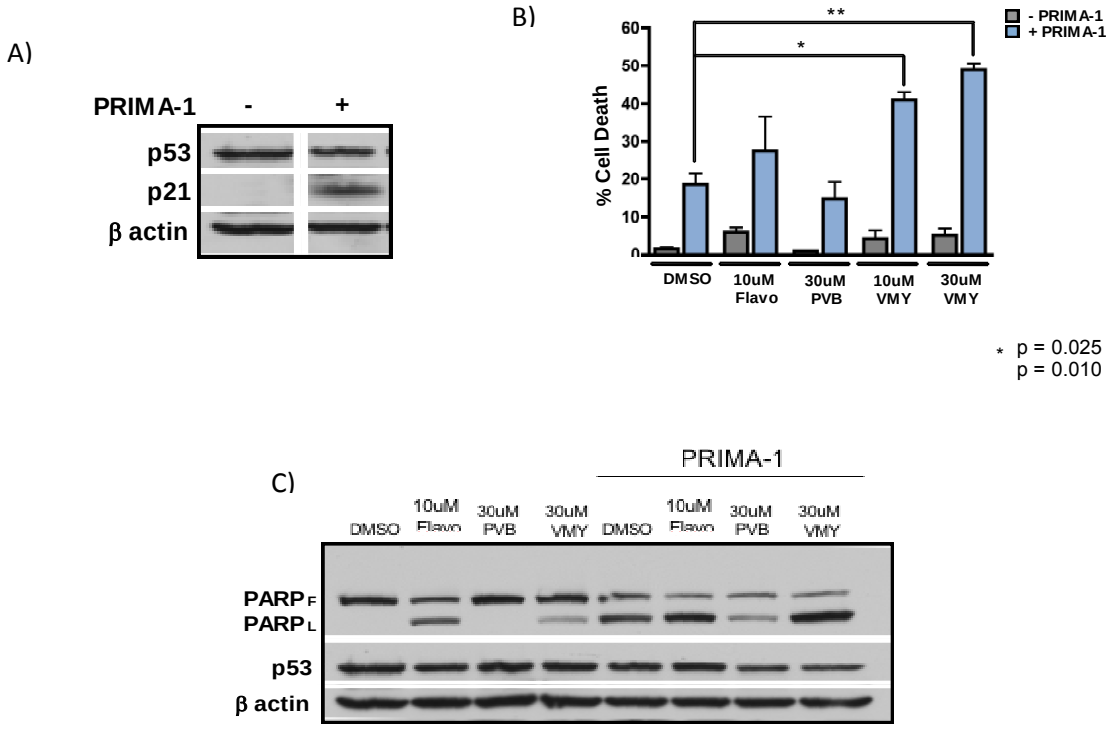

*Figure 4*: A) PRIMA-1 treatment in DU145 cells restores p53 as seen by induction of p21. B) PRIMA-1 pre-treatment of DU145 cells, followed by 18hr treatment with either flavopiridol, purvalanol B, or 10uM or 30uM VMY significantly increase the percentage of cell death as measured by trypan blue exclusion. C) PRIMA-1 treatment in DU145 cells increases levels of PARP cleavage following treatment with 30uM VMY.

Figure 5: Mutant p53 transfection in LNCaP cells does not effect knockdown of the wild-type protein.

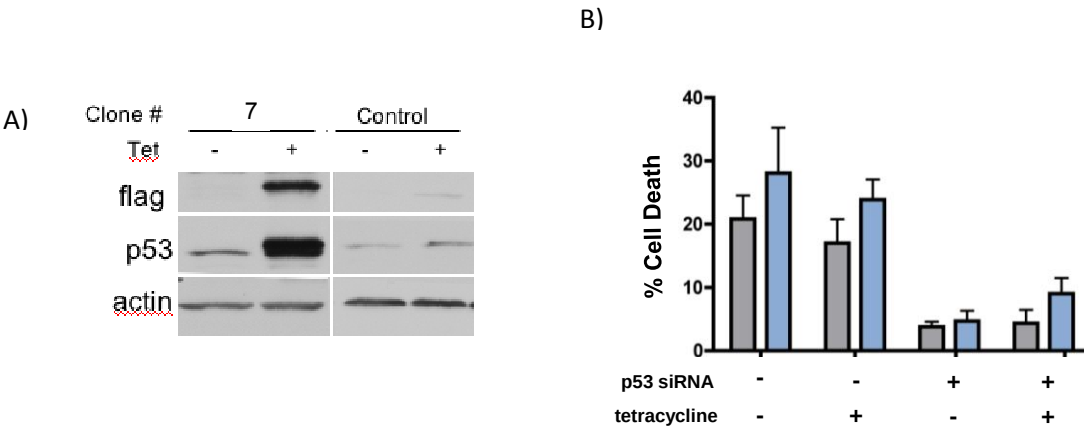


*Figure 5*: A) LNCaP cells were transfected with a tet-inducible p53 mutant (245) construct. Stable clones were selected using long-term G418 treatment and one representative clone is shown here. The construct is flag-tagged so flag protein and p53 levels increase upon addition of tetracycline in the stable population only. B) Percent cell death in LNCaP cells, as measured by subG1 content, increases upon 10uM and 30uM treatment versus DMSO treatment. Upon addition of p53 siRNA, VMY-mediated cell death is greatly reduced. Induction of the 245 mutant p53 construct via addition of tetracycline does not rescue the affect.

Cancer Biology & Therapy 10:4, 320-325; August 15, 2010; © 2010 Landes Bioscience

# VMY-1-103, a dansylated analog of purvalanol B, induces caspase-3-dependent apoptosis in LNCaP prostate cancer cells

Lymor Ringer,[1,†] Paul Sirajuddin,[1,†] Venkata Mahidhar Yenugonda,[1,3] Anup Ghosh,[1] Kyle Divito,[3] Valerie Trabosh,[3] Yesha Patel,[1,‡] Amanda Brophy,[1] Scott Grindrod,[1,3] Michael P. Lisanti,[4] Dean Rosenthal,[1,3] Milton L. Brown,[1,3] Maria Laura Avantaggiati,[1] Olga Rodriguez[1] and Chris Albanese[1,2,*]

[1]Lombardi Comprehensive Cancer Center and Department of Oncology; [2]Department of Pathology; and [3]Drug Discovery Program; Georgetown University Medical Center; Washington, DC USA; [4]Kimmel Cancer Center; Thomas Jefferson University; Philadelphia, PA USA

[‡]Current address: Marshall University Medical School; Huntington, WV USA

[†]These authors contributed equally to this work.

**Key words:** prostate cancer, apoptosis, cell cycle, CDK inhibitor, p53

The 2,6,9-trisubstituted purine group of cyclin dependent kinase inhibitors have the potential to be clinically relevant inhibitors of cancer cell proliferation. We have recently designed and synthesized a novel dansylated analog of purvalanol B, termed VMY-1-103, that inhibited cell cycle progression in breast cancer cell lines more effectively than did purvalanol B and allowed for uptake analyses by fluorescence microscopy.

ErbB-2 plays an important role in the regulation of signal transduction cascades in a number of epithelial tumors, including prostate cancer (PCa). Our previous studies demonstrated that transgenic expression of activated ErbB-2 in the mouse prostate initiated PCa and either the overexpression of ErbB-2 or the addition of the ErbB-2/ErbB-3 ligand, heregulin (HRG), induced cell cycle progression in the androgen-responsive prostate cancer cell line, LNCaP.

In the present study, we tested the efficacy of VMY-1-103 in inhibiting HRG-induced cell proliferation in LNCaP prostate cancer cells. At concentrations as low as 1 μM, VMY-1-103 increased both the proportion of cells in $G_1$ and $p21^{CIP1}$ protein levels. At higher concentrations (5 μM or 10 μM), VMY-1-103 induced apoptosis via decreased mitochondrial membrane polarity and induction of p53 phosphorylation, caspase-3 activity and PARP cleavage. Treatment with 10 μM Purvalanol B failed to either influence proliferation or induce apoptosis.

Our results demonstrate that VMY-1-103 was more effective in inducing apoptosis in PCa cells than its parent compound, purvalanol B, and support the testing of VMY-1-103 as a potential small molecule inhibitor of prostate cancer in vivo.

## Introduction

The cyclins are regulatory proteins that modulate the activity of the cyclin-dependent kinases (Cdks), thereby directing the orderly progression of eukaryotic cells through the cell cycle, ultimately resulting in normal cellular division.[1] The deregulation of various multi-protein cyclin/Cdk complexes has been described in many types of human tumors, including prostate cancer.[2]

The development of small molecules that inhibit the activity of cyclin/Cdk complexes has gained attention recently as technological advances in drug design have lead to improved target selectivity. The 2,6,9-trisubstituted purine group of cyclin dependent kinase inhibitors, which includes roscovitine and the purvalanols,[3] act by selectively competing with ATP at its binding site in targeted CDK's. We have recently described the design and synthesis of a novel dansylated-fluorescent analog of purvalanol B, termed VMY-1-103.[4] The design of this compound took advantage of both the known crystal structure of the purvalanol B/Cdk2 complex, as well as the fact that the carboxylic acid of the 6-anilino group of purvalanol can be modified without negatively affecting the chemicals ability to compete at the CDK ATP binding site. By synthetically coupling the fluorescent compound dansyl-ethylenediamine to purvalanol B, we found that VMY-1-103 inhibited cell cycle progression and increased apoptosis in breast cancer cell lines more effectively than purvalanol B. Since the dansyl group rendered the compound more lipophilic, we hypothesize that VMY-1-103 has an enhanced ability to diffuse through the cell membrane, increasing its cytoplasmic bioavailability.[4]

*Correspondence to: Chris Albanese; Email: Albanese@georgetown.edu
Submitted: 04/28/10; Accepted: 05/03/10
Previously published online: www.landesbioscience.com/journals/cbt/article/12208
DOI: 10.4161/cbt.10.4.12208

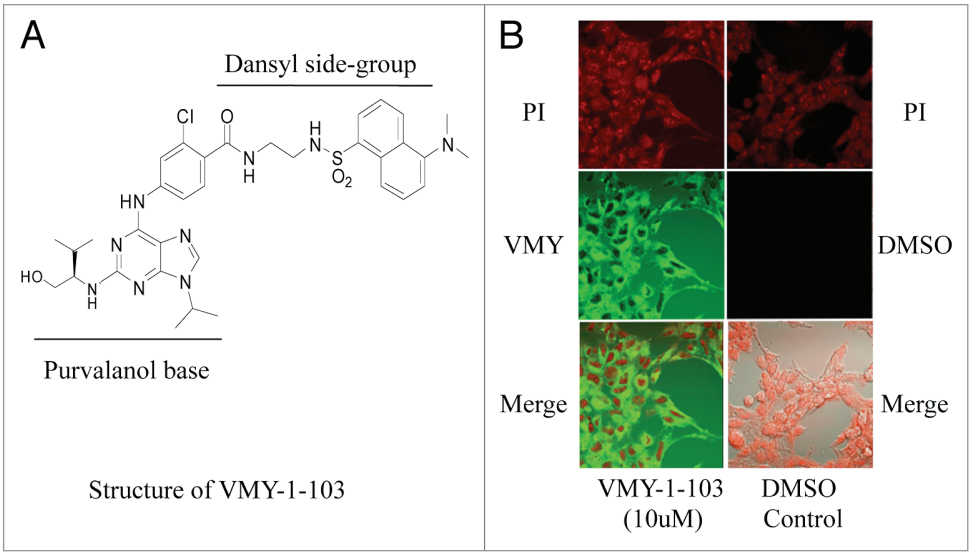


**Figure 1.** (A) Structure of VMY-1-103. (B) Uptake and subcellular localization of VMY-1-103 in LNCaP cells. PI, propidium iodide.

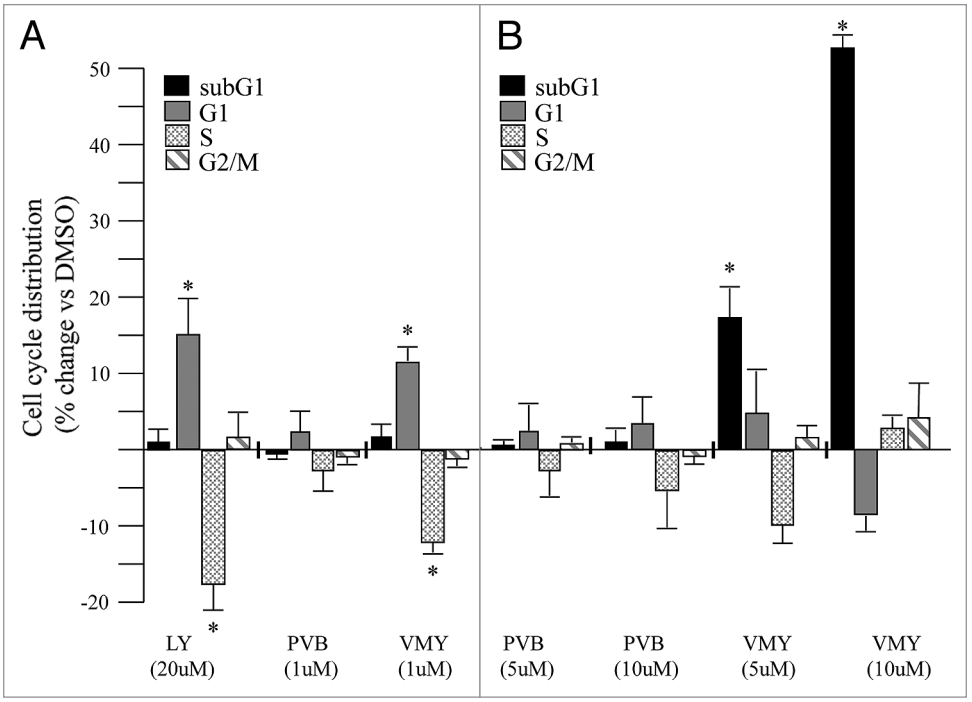


**Figure 2.** VMY-1-13 regulation of cell cycle progression and apoptosis in the human prostate cancer cell line LNCaP. Effect of LY294002 (LY), purvalanol B (PVB) or VMY-1-103 (VMY) on HRG-induced cell cycle progression and subG$_1$-phase associated apoptosis at (A) low and (B) high concentrations (5–10 μM). Values are percent change (average ± SD, N = 3) versus cells treated with the vehicle, DMSO. Asterisk, $p \leq 0.05$.

Our previous work has established that increased ErbB-2 signaling combined with the loss of one *pten* allele can initiate epithelial neoplasia in the mouse prostate that progresses to PCa commensurate with an induction of PI3-kinase/PDK1 signaling.[2,5,6] We have also shown that ErbB-2 and the ErbB-2/ErbB-3 ligand heregulin (HRG) induced cell cycle progression in PCa cells in part through induction of cyclin D1.[2] Since we have data establishing that VMY-1-103 inhibited cell cycle progression in MCF7 cells,[4] we tested the ability of VMY-1-103 to inhibit HRG-induced proliferation in the androgen-sensitive prostate cancer cell line, LNCaP. In this report, we present evidence that VMY-1-103 at concentrations as low was 1 μM increased the proportion of HRG-stimulated LNCaP cells arresting in the G$_1$ phase of the cell cycle. Additionally, VMY-1-103 at 5 μM and 10 μM significantly induced p53 phosphorylation and apoptosis and decreased cell viability in a manner that was caspase-dependent.

## Results

**VMY-1-103 inhibits heregulin-induced cell cycle progression in LNCaP cells.** We have recently described the design and synthesis of a novel dansylated-analog of purvalanol B, termed VMY-1-103 (**Fig. 1A** and reviewed in ref. 4). Incubation of prostate cancer LnCAP cells with 10 μM VMY-1-103 for 12 h resulted in more than 95% of percent of the cells containing cytoplasmic VMY-1-103 (**Fig. 1B**).

Since HRG induced cell cycle progression in LNCaP cells,[2] we next tested the ability of VMY-1-103 to inhibit HRG-induced proliferation in LNCaP cells. Treatment with 1 ng/ml heregulin and either 20 μM LY294002 or 1 μM VMY-1-103 for 18 hours resulted in a significant increase in the number of cells in G$_1$ and a concomitant decrease in the number of cells in S-phase (**Fig. 2A**). Purvalanol B (1 μM) had no effect (**Fig. 2A**). Similar results were seen in the presence of serum (**Suppl. Fig. 1**).

**VMY-1-103 induces apoptosis in LNCaP cells.** We next tested if higher concentrations of either purvalanol B or VMY-1-103 had any differential effects on cell cycle progression. Treatment of LNCaP cells with either 5 μM or 10 μM purvalanol B failed to significantly alter cell cycle progression or increase the sub-G$_1$ population of apoptotic cells (**Fig. 2B**). In contrast, 5 and 10 μM VMY-1-103 produced significant dose-dependent increases in the sub-G$_1$ population of apoptotic cells, however the G$_1$ arrest observed at 1 μM was lost

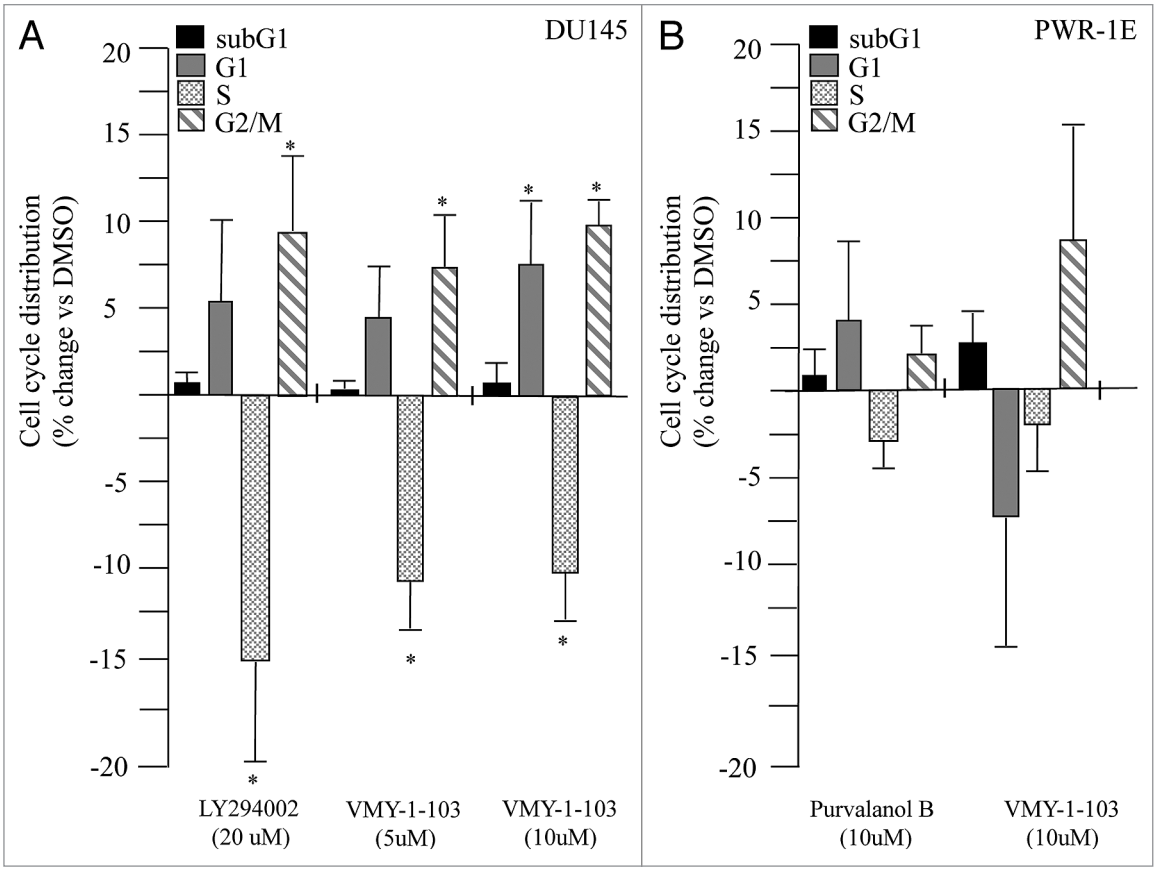


**Figure 3.** (A) Effect of VMY-1-103 on cell cycle progression and subG$_1$-phase associated apoptosis in (A) DU145 cells treated with HRG, (B) PWR-1E cells treated with HRG. Values are percent change (average ± SD, N = 3) versus cells treated with the vehicle, DMSO. Asterisk, $p \leq 0.05$.

(**Fig. 2B**). Experiments performed on DU145 cells demonstrated that while VMY-1-103 at 10 μM increased the proportion of cells in $G_1$ and $G_2$/M, and decreased the S-phase fraction, there was no significant change in the sub-$G_1$ population of apoptotic cells (**Fig. 3A**). Likewise, 10 μM VMY-1-103 did not significantly increase the sub-$G_1$ population of cells in the immortalized prostate epithelial cell line PWR-1E (**Fig. 3B**).

**VMY-1-103 induces apoptosis via induction of p53, caspase-3 activity and PARP cleavage.** In order to begin to investigate the mechanisms by which VMY-1-103 regulated apoptosis, antibody proteomic arrays were performed. Treatment of HRG-stimulated LNCaP cells with 10 μM VMY-1-103 significantly increased phosphorylation of p53 at serine residues 15, 46 and 392 (**Fig. 4A and B**), while LY294002 or 1 μM VMY-1-103 had only modest effects versus DMSO control. In addition, 10 μM VMY-1-103 significantly increased the levels of cleaved caspase-3 ("c-casp-3"), the active form generated by proteolytic maturation (**Fig. 4**). Western blotting further revealed dose-dependent increases in PARP-cleavage and levels of the Cdk inhibitor, $p21^{CIP1}$ (**Fig. 4C**). The levels of the late-$G_1$-phase cell cycle regulatory protein cyclin E were unaffected (**Fig. 4C**), suggesting the cells had undergone a switch from a VMY-1-103-induced cell cycle arrest to apoptosis.

**Apoptosis induced by VMY-1-103 is associated with early mitochondrial membrane depolarization.** During apoptosis, mitochondria undergo changes in membrane permeability that result in its depolarization. To further explore the mechanisms by which VMY-1-103 affected cell viability, mitochondrial polarity measurements were performed using Mitotracker Red CMXRos and flow cytometry. Addition of 10 μM VMY-1-103, but not 10 μM purvalanol B, resulted in statistically significant decreases in mitochondrial membrane polarity by 45 minutes of treatment (**Fig. 5A**). These results indicated that mitochondrial depolarization is an early apoptosis-inducing event following VMY-1-103 treatment. Caspase-3 activity, as measured by Z-DEVD-AMC catalysis, was also significantly induced by 10 μM VMY-1-103 (**Fig. 5B**).

**VMY-1-103 modulates components the intrinsic apoptotic pathway in LNCaP cells.** To assess the role that the intrinsic pathway plays in VMY-1-103-induced apoptosis, the caspase-9 inhibitor Z-LEHD-FMK was used. LNCaP cells were treated with Z-LEHD-FMK or DMSO for 1 hour, followed by 12 hrs of HRG and either DMSO or VMY-1-103. Z-LEHD-FMK significantly reduced the VMY-1-103-induced cell death as measured by trypan blue dye exclusion (**Fig. 5C**).

Mechanistically, these data establish that 1 μM VMY-1-103-induced $G_1$ arrest in LNCaP cells, perhaps in part through an induction of $p21^{CIP.1}$ At 10 μM, VMY-1-103 induced components of the intrinsic apoptotic pathway, linking mitochondrial membrane depolarization and alterations in p53 phosphorylation at multiple residues to increased caspase-3 activity and PARP cleavage.

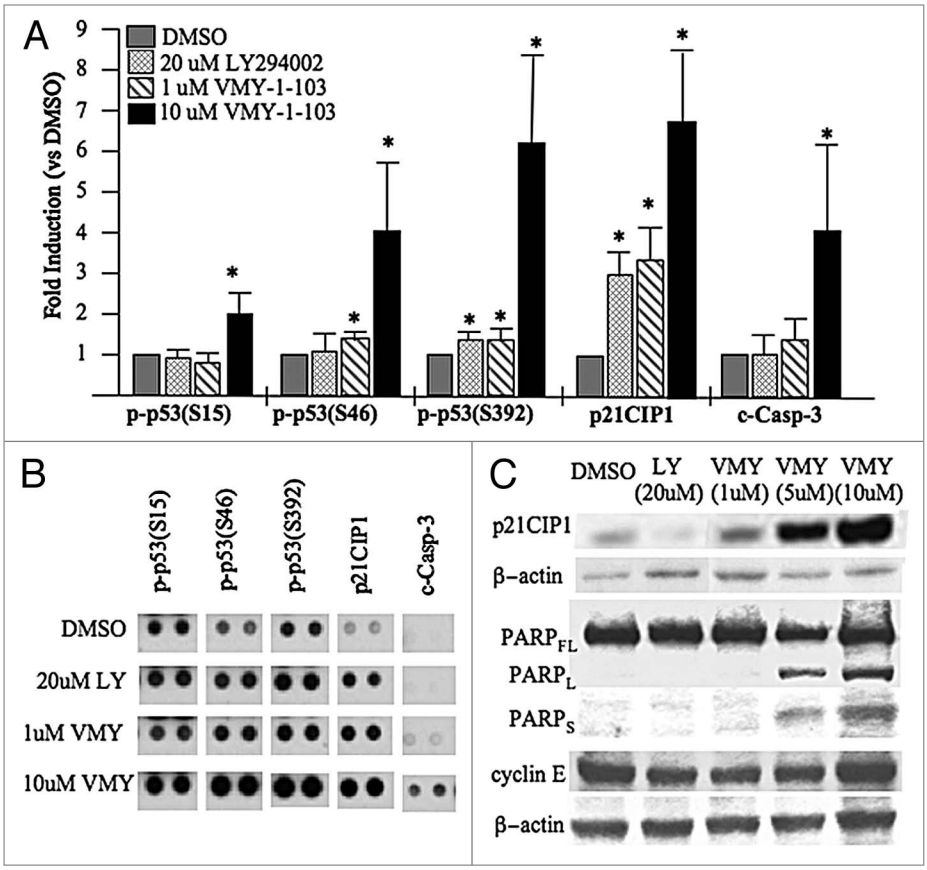


**Figure 4.** Activation of pro-apoptotic signaling by VMY-1-103. (A) Regulation of serine phosphorylation of the tumor suppressor protein, p53 (p-p53) as well as levels of $p21^{CIP1}$ and cleaved caspase-3 (c-casp-3) in LNCaP cells treated with HRG and either 20 μM LY294002, 1 μM VMY-1-103 or 10 μM VMY-1-103. Data are fold induction ± SE (N = 4 measurements). (B) Representative data from the antibody microarrays. (C) Western blot showing induction of $p21^{CIP1}$ levels and PARP cleavage by VMY-1-103. The FL, L and S subscripts stand for full-length PARP or the long and short cleaved fragments, respectively. Asterisk, $p \leq 0.05$.

## Discussion

Accumulating evidence has demonstrated that the purine-substituted family of CDK-inhibitors, such as purvalanol B, have the potential to be useful cancer therapeutics, however the mechanisms by which they regulate cell function has not been entirely elucidated.

In the present report, we examined the effects of a danslylated purvalanol B analog, VMY-1-103, on cell cycle progression and apoptosis in LNCaP prostate cancer cells. VMY-1-103 inhibited HRG-induced cell cycle progression at the $G_1$ phase at 1 μM, and severely reduced cell viability at 10 μM, resulting in a greater than 25% increase in death as measured by trypan blue dye exclusion. VMY-1-103 at 10 μM also induced mitochondrial membrane depolarization, and pathway analyses established that VMY-1-103 increased levels of cleaved caspase-3 (**Fig. 4**) and reduced the levels of cIAP-1 and XIAP (Ringer L and Albanese C, unpublished). The loss of cell viability was significantly attenuated by the caspase-9 inhibitor, implicating activation the intrinsic apoptotic pathway by VMY-1-103, resulting in the eventual activation of caspase-3 and PARP cleavage.

Increased nuclear p53 levels, resulting from increased protein levels or somatic mutations, correlate with increased clinical PCa grade and Gleason scores. Our studies revealed that VMY-1-103 at 10 μM induced the phosphorylation levels at serine (Ser) residues 15, 46 and 392 on p53. Activation of p53 can lead to cell cycle arrest, apoptosis or senescence. p53-Ser15 is a target of ATR[7] and phosphorylation of p53 on Ser15 stabilizes the protein by preventing interactions with Mdm2 and subsequent ubiquitination. Phosphorylation of p53-Ser392 increases the stability of the p53 tetramerization domain.[8] Ck2 and SSRP1,[9] target Ser392 for phosphorylation and p38/MAPK can also phosphorylate p53 on Ser392, promoting $G_2$ arrest and/or p53-mediated apoptosis. p38/MAPK and HIPK2 phosphorylate p53 on Ser46, thereby mediating apoptosis through p53 apoptosis-inducing protein 1 ($p53^{AIP1}$).[9] Phosphorylation of p53 at Ser15 is associated with increased levels of $p21^{CIP1}$.[1,10] Interestingly, however, induction of $p21^{CIP1}$ was observed at both low and high levels of VMY-1-103, while p53 Ser15-phosphorylation was only observed at higher doses of VMY-1-103. Our results indicate that Ser15 phosphorylation may not be required for transcriptional induction of *$p21^{CIP}$*.[1] The $p21^{CIP1}$ protein has been shown to function either as a pro- or anti-apoptotic factor in numerous other studies,[11] whether the increased $p21^{CIP1}$ levels and the altered phosphorylation status of p53 contribute individually or in combination to activating the intrinsic apoptotic pathway remains to be determined.

We also found that VMY-1-103 was far less effective in inducing apoptosis in prostate cells with compromised p53 function (**Fig. 3**). DU145 PCa cells express a mutant p53 and the noncancerous PWR-1E cell line was immortalized with SV40, which inhibits p53 function and these exhibit predominantly nuclear p53.[12] In addition, VMY-1-103 failed to increase apoptosis in the p53-null cell line, PC3 (Ringer L and Albanese C, unpublished). Further experiments will be required to establish whether knockdown of p53 desensitizes LNCaP cells to VMY-103, or conversely whether the re-expression of wildtype-p53 restores sensitivity in to VMY-1-103 in DU145 or PC3 cells.

We have shown that VMY-1-103 is an effective anti-tumor compound, especially given its rapid pro-apoptotic effect in LNCaP cells. The addition of a dansyl group both rendered the chemical more biologically active than purvalanol B in vitro and enabled the imaging of VMY-1-103 uptake by confocal microscopy. Our data indicate that VMY-1-103 therefore may be useful

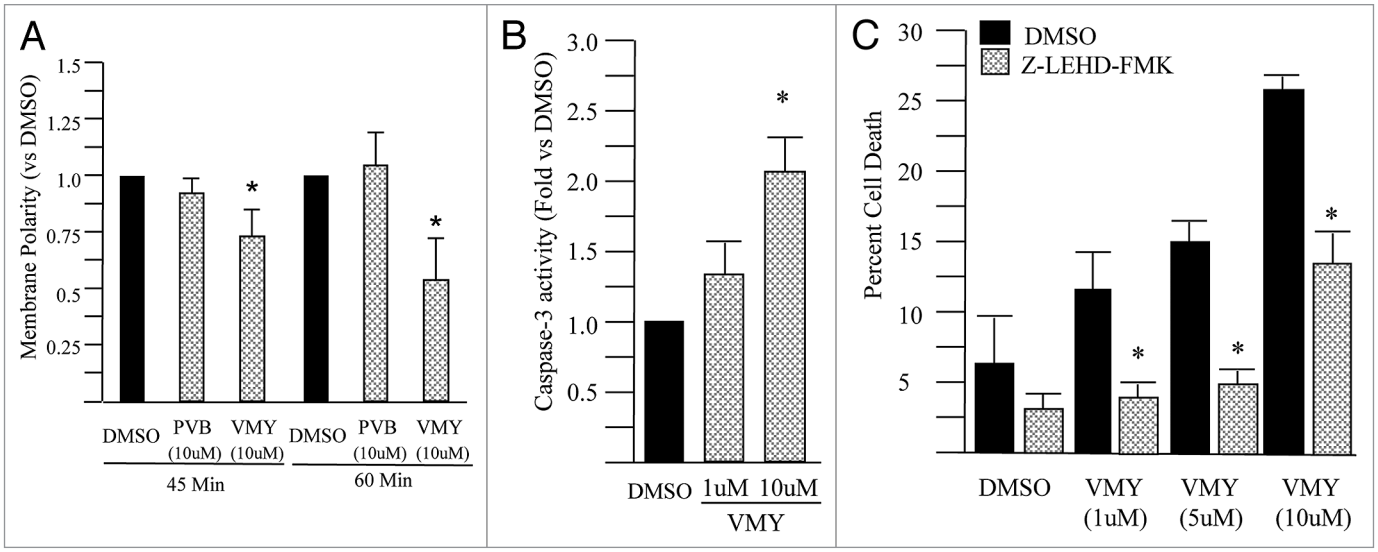


**Figure 5.** Capsase activity in HRG stimulated LNCaP cells treated with VMY-1-103. (A) Effects of 10 μM purvalanol B (PVB) or VMY-1-103 (VMY) on mitochondrial membrane polarity. Data are percent change vs. DMSO control. (B) VMY-1-103 induced caspase-3 activity was measured fluorometrically using the caspase-3 substrate, Z-DEVD-AMC. Data are fold increase (±SE) versus DMSO treated cells (N = 4). (C) Abrogation of VMY-1-103 induced apoptosis through inhibition of capsase-9 via Z-LEHD-FMK. Data are average percent change in trypan blue positive cells (±SD, N = 3) of cells treated with increasing amounts of VMY-1-103 and either DMSO (black bars) or 20 μM Z-LEHD-FMK (hatched bars). Asterisk, $p \leq 0.05$.

for the treatment of at least a large subset of early prostate cancers that express wildtype p53, and preclinical studies will be performed to verify its in vivo delivery and biological efficacy in treating PCa. Importantly the dansylation will allow for the quantification of VMY-1-103's in vivo pharmacodymanics and tissue distribution by mass spectroscopy.

## Methods and Materials

**Cell lines and cell culture.** The human prostate cancer cell lines LNCaP and DU145 were maintained in RPMI and DMEM, respectively, with 10% FCS, 0.1 mM non-essential amino acids, 100 U/ml Penicillin-Streptomycin and 1 mM sodium pyruvate at 37°C in 5% $CO_2$ as previously described.[2,5,13] The non-tumorigenic, immortalized cell line, PWR-1E, was maintained in Keratinocyte Serum Free Medium (K-SFM, Life Technologies) supplemented with 0.05 mg/ml bovine pituitary extract and 5 ng/ml EGF. For heregulin 1β (HRG) stimulation studies, subconfluent (approximately 50%) LNCaP, DU145 or PWR-1E cells were treated with 1 ng/ml HRG (R&D Systems. Minneapolis, MN), as previously described.[2] The PI3K inhibitor LY294002 (20 μM), the parent CDK inhibitor purvalanol B (Sigma), or VMY-1-103 (**Fig. 1A**) at 1, 5 and 10 μM were added to the culture medium for up to 18 hours. DMSO was used as vehicle control.

**VMY-1-103.** The drug discovery program at Georgetown University Medical Center designed and synthesized (R)-2-chloro-N-(2-(5-(dimethylamino)naphthalene-1-sulfonamido) ethyl)-4-(2-(1-hydroxy-3-methylbutan-2-ylamino)-9-isopropyl-9H-purin-6-ylamino)benzamide or VMY-1-103.[4] Briefly, 2-chloro-N-(2-(5-(dimethylamino)naphthalene-1-sulfonamido) ethyl)-4-(2-fluoro-9-isopropyl-9H-purin-6-ylamino)benzamide (0.47 g, 0.75 mmol), R-(-)-2-amino-3-methyl-1-butanol (0.38 g, 3.76 mmol), and diisopropylethylamine (0.65 mL, 3.76 mmol) were dissolved in n-butanol and placed in a sealed tube. The reaction mixture was heated to 120°C for 24 h. After 24 h R-(-)-2-amino-3-methyl-1-butanol (1.88 mmol) and diisopropylethylamine (1.88 mmol) were added and the reaction was allowed to stir for an additional 48 h. The solvent was removed in vacuo and the crude product dissolved in $CH_2Cl_2$. The organic layer was washed with water (25 ml) three times followed by brine (50 mL). The organic layer was separated and dried over anhydrous sodium sulfate, filtered and concentrated under reduced pressure to give 0.300 g of crude product. The crude product was purified by column chromatography.

**Flow-cytometry.** The prostate cells were collected by trypsinization, fixed in 10% ethanol and resuspended in PBS containing 20 μg/ml propidium iodide (PI) and 5U RNase A. DNA content was measured using a FACStar Plus dual laser FACSort system (Becton-Dickinson) as previously described.[14,15]

**Immunoblotting.** Protein extracts were separated on 4–20% Tris-glycine gels and electro-blotted onto nitrocellulose.[2] Protein levels were assessed using antibodies against $P21^{CIP1}$ (Santa Cruz, sc481) PARP (Cell Signaling, 9542), or cyclin E (DCS60, Cell Signaling, 2946). Anti-β-actin (Cell Signaling, 4967) was used as loading control.

**Cell viability and growth.** Following inhibitor treatment, cell viability was determined by trypan blue exclusion. For the apoptosis assays, Proteome Profiler human apoptosis arrays (R&D Systems) were performed as described in the manufacture's protocol. Briefly, nitrocellulose membranes (spotted with 35 antibodies, in duplicate) were blocked with the array buffer (supplied by the manufacturer) for 1 hour at room temperature, the membranes were washed, and incubated with 500 μg of protein overnight at 4°C. Biotinylated primary antibody (supplied by the manufacturer)

was added for 1 hour, followed by a 30-minute incubation with Streptavidin-HRP, and finally ECL reagent (1:3,000; Pierce) solution. Array data was developed on x-ray film and spot areas and intensities were analyzed using ImageJ (NIH) software.

**Caspase-3 assays.** LNCaP cells were treated for 12 hours with VMY-1-103 and HRG after which protein was extracted. Protein extracts (25 μg) were adjusted to a final volume of 50 μl using lysis buffer. 50 μl of the caspase-3 substrate Z-DEVD-AMC (7-amino 4-methylcoumarin) was added to each sample in a 96 well plate. AMC accumulation, and thus caspase-3 activity, was measured every 3 minutes for 18 cycles using a Victor $^3$V cytofluorometer (Perkin Elmer) using 360/40 nm excitation and 460/40 nm emission filters. All caspase activity slopes were plotted graphically to ensure that reactions were proceeding at a linear rate for the time interval measured.

**Caspase-9 inhibition.** The irreversible caspase-9 inhibitor, Z-LEHD-FMK (Sigma; St. Louis, MO), was added to cells at a final concentration of 20 μM, 10 minutes prior to exposure to HRG and VMY-1-103. The cells were harvested at 12 hours and stained with trypan blue to determine cell viability.

**Mitochondrial membrane polarity.** 1 x $10^6$ LNCaP cells, treated with HRG and either DMSO or inhibitors, were incubated with 100 nM of Mitotracker Red CMXRos (Molecular Probes, Eugene, OR) for 45 or 60 minutes at 37°C. Mitochondrial membrane polarity was measured by flow cytometry using a FACStar Plus dual laser FACSort system (excitation at 579 nm, emission 599 nm).

**Fluorescent imaging.** LNCap cells were seeded on glass coverslips and treated with HRG and either DMSO or 10 μM VMY-1-103 for 18 h. Cells were washed with PBS and fixed in 10% formalin for 10 minutes. Cells were washed with PBS, stained with 0.1 μg/ml propidium iodide (BD Pharmingen) for 5 minutes, and washed with PBS an additional 3 times. The coverslips were mounted onto glass slides with Tris-buffered fluoro-gel (Electron Microscopy Sciences, Hatfield, PA). Multiphoton confocal microscopy was performed (Zeiss510LSM/META/NLO, 63X oil immersion) at 720 nm/480–520 nm (excitation/emission) for VMY-1-103 and 535 nm/617 nm (excitation/emission) for propidium iodide.


### Acknowledgements

Cell cycle analyses were performed in the Lombardi Cancer Center's Flow Cytometry shared resource. Fluorescence microscopy was performed in the Lombardi Cancer Center's Microscopy and Imaging Shared Resource.

Grant support, P30 CA51008, R01CA129003 (CA).


### Note

Supplementary materials can be found at:
www.landesbioscience.com/supplement/RingerCBT10-3-Sup.pdf

### References


1. Pestell RG, Albanese C, Reutens AT, Segall JE, Lee RJ, Arnold A. The cyclins and cyclin-dependent kinase inhibitors in hormonal regulation of proliferation and differentiation. Endocrine Rev 1999; 20:501-34.
2. Casimiro M, Rodriguez O, Pootrakul L, Aventian M, Lushina N, Cromelin C, et al. ErbB-2 induces the cyclin D1 gene in prostate epithelial cells in vitro and in vivo. Cancer Res 2007; 67:4364-72.
3. Chang YT, Gray NS, Rosania GR, Sutherlin DP, Kwon S, Norman TC, et al. Synthesis and application of functionally diverse 2,6,9-trisubstituted purine libraries as CDK inhibitors. Chem Biol 1999; 6:361-75.
4. Yenugonda VM, Deb TB, Grindrod SC, Dakshanamurthy S, Yang Y, Paige M, et al. Design, synthesis and evaluation of fluorescent cyclin-dependent kinase inhibitors in human breast cancer cells. Submitted 2010.
5. Rodriguez OC, Lai EW, Vissapragada S, Cromelin C, Avetian M, Salinas P, et al. A reduction in Pten tumor suppressor activity promotes ErbB-2-induced mouse prostate adenocarcinoma formation through the activation of signaling cascades downstream of PDK1. Am J Pathol 2009; 174:2051-60.
6. Vissapragada S, Ghosh A, Ringer L, Salinas P, Brophy A, Peaceman D, et al. Dietary n-3 polyunsaturated fatty acids fail to reduce prostate tumorigenesis in the PB-ErbB-2 x Pten(+/-) preclinical mouse model. Cell Cycle 2010; 9:1824-9.
7. Bhattacharya S, Ray RM, Johnson LR. Role of polyamines in p53-dependent apoptosis of intestinal epithelial cells. Cell Signal 2009; 21:509-22.
8. Oren M, Rotter V. Introduction: p53—the first twenty years. Cell Mol Life Sci 1999; 55:9-11.
9. Keller DM, Lu H. p53 serine 392 phosphorylation increases after UV through induction of the assembly of the CK2.hSPT16.SSRP1 complex. J Biol Chem 2002; 277:50206-13.
10. Yagi A, Hasegawa Y, Xiao H, Haneda M, Kojima E, Nishikimi A, et al. GADD34 induces p53 phosphorylation and p21/WAF1 transcription. J Cell Biochem 2003; 90:1242-9.
11. Liu S, Bishop WR, Liu M. Differential effects of cell cycle regulatory protein p21(WAF1/Cip1) on apoptosis and sensitivity to cancer chemotherapy. Drug Resist Updat 2003; 6:183-95.
12. Webber MM, Bello D, Quader S. Immortalized and tumorigenic adult human prostatic epithelial cell lines: characteristics and applications. Part I. Cell markers and immortalized nontumorigenic cell lines. Prostate 1996; 29:386-94.
13. Rodriguez O, Fricke S, Chien C, Dettin L, Vanmeter J, Shapiro E, et al. Contrast-enhanced in vivo imaging of breast and prostate cancer cells by MRI. Cell Cycle 2006; 5:113-9.
14. Albanese C, D'Amico M, Reutens AT, Fu M, Watanabe G, Lee RJ, et al. Activation of the *cyclin D1* gene by the E1A-associated protein p300 through AP-1 inhibits cellular apoptosis. J Biol Chem 1999; 274:34186-95.
15. Albanese C, Wu K, D'Amico M, Jarrett C, Joyce D, Hughes J, et al. IKKalpha Regulates Mitogenic Signaling through Transcriptional Induction of Cyclin D1 via Tcf. Mol Biol Cell 2003; 14:585-99.

Cancer Biology & Therapy 12:9, 818-826; November 1, 2011; © 2011 Landes Bioscience

# VMY-1-103 is a novel CDK inhibitor that disrupts chromosome organization and delays metaphase progression in medulloblastoma cells

Lymor Ringer,[1] Paul Sirajuddin,[1] Mary Heckler,[1] Anup Ghosh,[1] Frank Suprynowicz,[2] Venkata M. Yenugonda,[3] Milton L. Brown,[1,3] Jeffrey A. Toretsky,[1] Aykut Uren,[1] YiChien Lee,[1] Tobey J. MacDonald,[4] Olga Rodriguez,[1] Robert I. Glazer,[1] Richard Schlegel[1,2] and Chris Albanese[1,2,*]

[1]Lombardi Comprehensive Cancer Center and Department of Oncology; [2]Department of Pathology; [3]Drug Discovery Program; Georgetown University Medical Center; Washington DC; [4]Department of Pediatrics; Emory University School of Medicine; Atlanta, GA USA

**Keywords:** medulloblastoma, apoptosis, mitotic catastrophe, CDK inhibitor, mitosis, cell cycle

Medulloblastoma is the most prevalent of childhood brain malignancies, constituting 25% of childhood brain tumors. Craniospinal radiotherapy is a standard of care, followed by a 12 mo regimen of multi-agent chemotherapy. For children less than 3 y of age, irradiation is avoided due to its destructive effects on the developing nervous system. Long-term prognosis is worst for these youngest children and more effective treatment strategies with a better therapeutic index are needed. VMY-1-103, a novel dansylated analog of purvalanol B, was previously shown to inhibit cell cycle progression and proliferation in prostate and breast cancer cells more effectively than purvalanol B. In the current study, we have identified new mechanisms of action by which VMY-1-103 affected cellular proliferation in medulloblastoma cells. VMY-1-103, but not purvalanol B, significantly decreased the proportion of cells in S phase and increased the proportion of cells in $G_2$/M. VMY-1-103 increased the sub $G_1$ fraction of apoptotic cells, induced PARP and caspase-3 cleavage and increased the levels of the Death Receptors DR4 and DR5, Bax and Bad while decreasing the number of viable cells, all supporting apoptosis as a mechanism of cell death. $p21^{CIP1/WAF1}$ levels were greatly suppressed. Importantly, we found that while both VMY and flavopiridol inhibited intracellular CDK1 catalytic activity, VMY-1-103 was unique in its ability to severely disrupt the mitotic spindle apparatus, significantly delaying metaphase and disrupting mitosis. Our data suggest that VMY-1-103 possesses unique antiproliferative capabilities and that this compound may form the basis of a new candidate drug to treat medulloblastoma.

## Introduction

During brain development and maturation, and in anticipation of populating the cerebral cortex with granular neurons, a burst of postnatal granular neuronal precursor cell proliferation occurs in the external granular layer of the brain. Following this period of rapid precursor cell expansion, an orderly exit from the cell cycle and coordinated migration and differentiation is required to direct the proper formation of the granular layer of the cerebellum, and a failure of normal differentiation and migration of the granular precursor cells is believed to be the cellular basis for a majority of medulloblastomas (MB) (reviewed in ref. 1). While locally advanced MB can have profound effects per se, one of the underlying clinical challenges related to MB treatment is its proclivity to spread throughout the neuraxis. Therefore, craniospinal radiotherapy is a standard of care delivered to children immediately after surgical resection of the tumor, followed by a 12 mo regimen of intensive multi-agent chemotherapy. While effective, this course of treatment has serious consequences. For example, a majority of survivors are left with auditory and growth deficits, and recent studies have demonstrated that irradiation significantly lowers cognitive development and function in 9 of the 12 intelligence subtest categories studied (reviewed in ref. 2). Irradiation is therefore avoided in children less than three years old due to its destructive effects on the developing nervous system. Long-term prognosis for these children is considerably worse and significant effort is underway to develop more effective MB treatment strategies.[3]

The etiology of MB is complex, and the heterogeneity of the tumors that arise is partially understood via identified alterations in genes and signaling pathways that either direct cell expansion or inhibit proliferation. Clinically, MBs have been assigned to five pathologically defined subtypes, and molecular profiling has further subclassified the tumors based on gene expression patterns and chromosomal abnormalities.[4-6] Dysregulation of Hedgehog (Hh) signaling, defined as the c3 MB subgroup,[6] is the most frequent developmental signaling pathway alteration in MBs, being found at the highest frequency in both children under 3 y of age

*Correspondence to: Chris Albanese; Email: albanese@georgetown.edu
Submitted: 07/28/11; Revised: 08/06/11; Accepted: 08/09/11
DOI:10.4161/cbt.12.9.17682

and in all MB patients over the age of 25.[6] Hh-associated MB tumors contain changes in the abundance of multiple proteins involved in cell cycle regulation, including Gli, cyclins D1 and D2 as well as N-Myc.[7] Similarly, a Myc activation signature is a defining characteristic of the c1 subgroup, and this group shows the worst overall survival, followed by the c3/Hh subgroup. The human MB cell lines, DAOY and D556 resemble the c3 and c1 subgroup, respectively, as maintenance of activated Smo signaling[8] and Gli transactivation[9] is required for DAOY cell proliferation, while D556 cells have amplified Myc.[10]

Regardless of the underlying cause, the tumors that form are highly proliferative, and more effective clinical treatments will require developing therapies that target critical components of the cell proliferation machinery.

The cyclins are regulatory proteins that modulate the activity of the cyclin-dependent kinases (Cdks), thereby directing the orderly progression of eukaryotic cells through the cell cycle.[11] Because of the prominent loss of normal cell cycle control and due to the extensive proliferation that is associated with MB, we anticipate that the ability to treat MB may be enhanced through identifying small molecule inhibitors that target critical components of the cell cycle regulatory machinery.[9] The 2,6,9-trisubstituted purine group of cyclin dependent kinase inhibitors act by competing with ATP in targeted CDK's.[12] We have recently developed a novel purvalanol B (PVB)-based small molecule inhibitor termed VMY-1-103 (VMY). This compound was synthesized with 6-anilino position coupling of a dansyl ethylenediamine group to both retain CDK-inhibitory function and enable fluorescent imaging capability.[13,14] We established that VMY exhibited a significant increase in potency vs. PVB in inducing cell cycle arrest and apoptosis in human prostate and breast cancer cell lines while still remaining largely inactive in immortalized cells, consistent with this group of inhibitors.[13,14] We believe that the increased potency of VMY may be due in part to the lipophilic dansyl side-group supporting increased cell membrane permeability. In the present study using human medulloblastoma cell lines, we present data that further establishes that VMY exhibits increased potency at inducing $G_2$/M arrest and in inducing apoptosis, PARP- and caspase-3-cleavage and increasing the levels of DR4, DR5, Bax and Bad vs. its parent compound, PVB. Importantly, we also present new findings demonstrating that while VMY was as effective as flavopiridol at inhibiting intracellular CDK1 enzymatic activity, achieving a greater than 90% inhibition, only VMY disturbed centrosome polarity, affecting chromosomal alignment and migration, thereby significantly disrupting mitosis. Our results indicate that VMY has unique properties related to its ability to rapidly disrupt the mitotic apparatus, potentially differentiating VMY from other small molecule CDK inhibitors.

## Results

**VMY inhibits cell cycle progression in DAOY.** We have recently described the effects of VMY, a novel dansylated-analog of purvalanol B on prostate and breast cancer cell lines.[13,14] In the present study, DAOY and D556 human medulloblastoma cell lines were utilized to assess the effect of VMY on MB cell cycle progression. DAOY cells were treated for 18 h with purvalanol B (PVB) or VMY at varying concentrations, or LY294002 at 20 uM as a control for cell cycle arrest (**Fig. 1A**). Treatment with LY294002 resulted in an increase in the number of cells in $G_1$ and a concomitant decrease in the number of cells in S-phase. PVB had no significant effect (**Fig. 1A**). Conversely, VMY significantly affected a $G_2$/M arrest beginning at 1 uM, which increased as the dose was escalated. Similar results were seen using the CDK inhibitor, flavopiridol (not shown). VMY treatment also increased the sub$G_1$ population of cells, consistent with DNA fragmentation and apoptotic cell death following treated with VMY. Treatment of DAOY cells with either LY294002 or PVB failed to significantly alter the sub-$G_1$ population of cells (**Fig. 1A**). Similar results were seen in D556 cells, with VMY inducing a significant $G_2$/M arrest beginning at 0.5 uM and an increased sub$G_1$ fraction beginning at 5.0 uM (**Fig. 1B**). Both VMY and the CDK inhibitor flavopiridol, but neither PVB nor the dansyl group alone, significantly induced cell death in DAOY cells at 18 h as measured by trypan blue dye exclusion (**Fig. 2A**). Furthermore, VMY had no effect on cell cycle progression or apoptosis in NIH3T3 cells (**Fig. S1A**), similar to our previous results in non-transformed prostate and breast cancer cell lines.[13,14] The $ED_{50}$'s (effective doses necessary to achieve 50% cell death) for VMY and flavopiridol were approximately 76 and 30.5 uM, respectively (**Fig. S1B and C**)

**VMY induces apoptosis via increased levels of pro-apoptotic proteins and caspase activity.** Using antibody proteome arrays we previously reported that VMY induced apoptosis in LNCaP prostate cancer cells in part through an induction of p53 and the intrinsic apoptotic pathway.[13] To investigate the mechanisms by which VMY regulated apoptosis in DAOY cells, similar experiments were performed. VMY significantly increased the protein levels of the death receptors DR4 and DR5, which are required for TRAIL-dependent induction of apoptosis in cancer cells. Levels of the Fas ligand TNFSF6 and cleaved caspase-3 (c-casp-3), the active form generated by proteolytic maturation, were also increased (**Fig. 2B**). The phosphorylation status of p53 serine residues 15, 46 and 392, which were induced by VMY in LNCaP cells,[13] were unaffected in DAOY cells (not shown). Levels of the proapoptotic proteins BAD and BAX were induced while levels of the antiapoptotic regulatory protein cIAP/Birc2 were modestly reduced (**Fig. 2B**).

Protein gel blots were run to assess the effect of VMY on levels of the CDK inhibitory protein $p21^{CIP1/WAF1}$, of cyclins E and B1 as well as PARP status (**Fig. 2C**). VMY, but not PVB, significantly increased the levels of cleaved PARP while levels of the $G_1$/S protein, cyclin E, were not changed. Surprisingly, while $p21^{CIP1}$ levels which were induced by VMY in LNCaP cells[13] and by low concentrations of VMY in DAOY cells (**Fig. 2C**), decreased by 82% (±3, n = 3) and 90% (±7, n = 3) with 10 and 30 μm VMY, respectively (**Fig. 2C**). Treatment with flavopiridol also significantly decreased $p21^{CIP1/WAF1}$ (**Fig. S1D**). The levels of cyclin B were marginally reduced by VMY at 10 and 30 uM (**Fig. 2C**).

**VMY inhibits CDK1 activity in DAOY cells.** Our recent data using purified cyclin/CDK complexes established that VMY was a potent inhibitor of the cyclinB/CDK1 complex.[14]

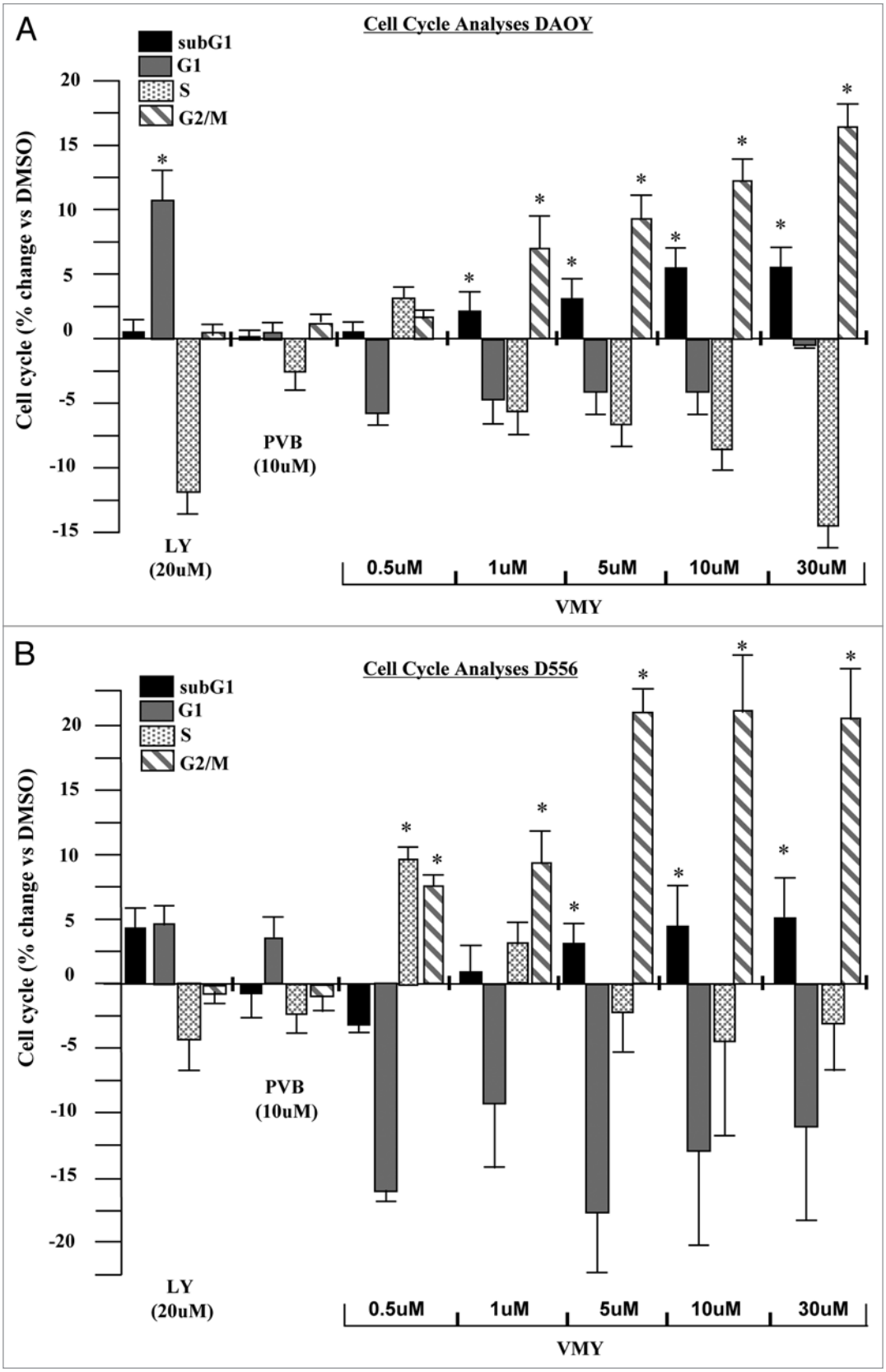


**Figure 1.** Effects of VMY on cell cycle progression in human medulloblastoma cells. The human medulloblastoma cell lines (A), DAOY or (B) D556 were treated for 18 h with either LY294002 (LY), purvalanol B (PVB) or VMY at the concentrations shown. Cells were harvested and both DNA fragmentation (subG$_1$) and the cell cycle profile were measured by flow cytometry. Data are average ± standard deviation of n ≥ three separate experiments vs. DMSO.

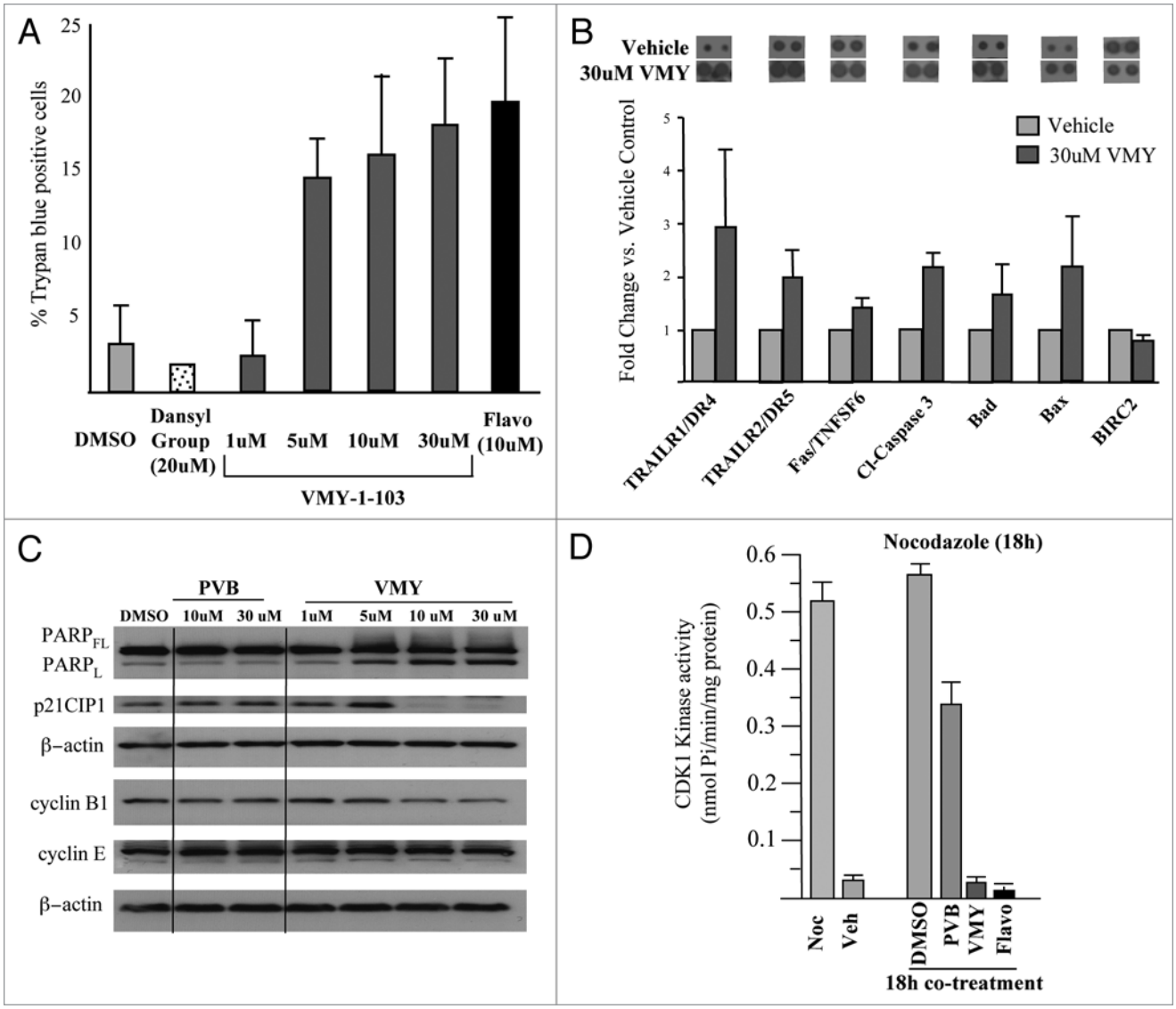


**Figure 2.** Effects of VMY on DAOY cell proliferation. (A) DAOY cells were treated for 18 h with either DMSO, the dansyl group alone or VMY-1-103 at the concentrations shown. Cells were harvested and cell viability assessed by trypan blue dye exclusion on >300 cells. Data are average ± standard deviation of n ≥ three separate experiments. (B) Apoptosis proteome arrays performed on extracts from DAOY cells were treated for 18 h with either DMSO or VMY at 30 uM. Fold change in protein abundance vs. DMSO are shown as Ave ± deviation of duplicate samples from n = two separate experiments. A representative proteomic array is shown at top. (C) Representative protein gel blot (n ≥ 3) performed on DAOY cells treated for 18 h with either PVB or VMY at the concentrations shown. (D) In vitro CDK1-kinase assays performed on DAOY cell extracts treated as marked. Data are percent inhibition in substrate phosphorylation vs. vehicle control for n = two experiments. Flavo, Flavopiridol; Cl$^{-}$ capase-3, cleaved caspase-3; PARP$_{FL}$, full length PARP; PARP$_{L}$, 89 kD fragment of cleaved PARP; Noc, nocodazole; Veh, vehicle.

We therefore assessed the CDK-inhibitory capacity of VMY in protein extracts from treated DAOY cells. The catalytic activity of CDK1 in the cell extract was assessed using an in vitro kinase reaction with the CDK1 peptide target substrate (ADA QHA TPP KKK RKV ED). Intracellular CDK1 activity was initially quantified using extracts from randomly cycling cells or in cells synchronized in the $G_2$-phase of the cell cycle with nocodazole. The CDK1-kinase activity in randomly cycling cells was less than 0.1 nmol of phosphate utilized per minute (0.035 nmol/min/mg ± 0.005, n = 3), which increased 15-fold in cells synchronized with nocodazole (to 0.522 nmol/min/mg ± 0.3, n = 4) (**Fig. 2D**). CDK1-kinase assays were next performed on extracts from DAOY cells co-treated for 18 h with nocodazole and either DMSO, PVB (30 um), VMY (30 um) or flavopiridol (10 uM). Both VMY and flavopiridol inhibited CDK1 activity by over 90% (**Fig. 2D**), vs. a 33% inhibition by PVB.

**VMY delays progression through mitosis.** Orderly regulation of the cyclinB/CDK1 complex is required for entry into mitosis.[15] As VMY was able to significantly inhibit CDK1 activity in DAOY cells, we next assessed whether a component of VMY's antiproliferative activity was associated with an inhibition of mitotic progression. To help determine how VMY blocked cell division, DAOY cells were stably transfected with histone-H2B-GFP (DAOY/H2B-GFP, described in the Methods section) to enable

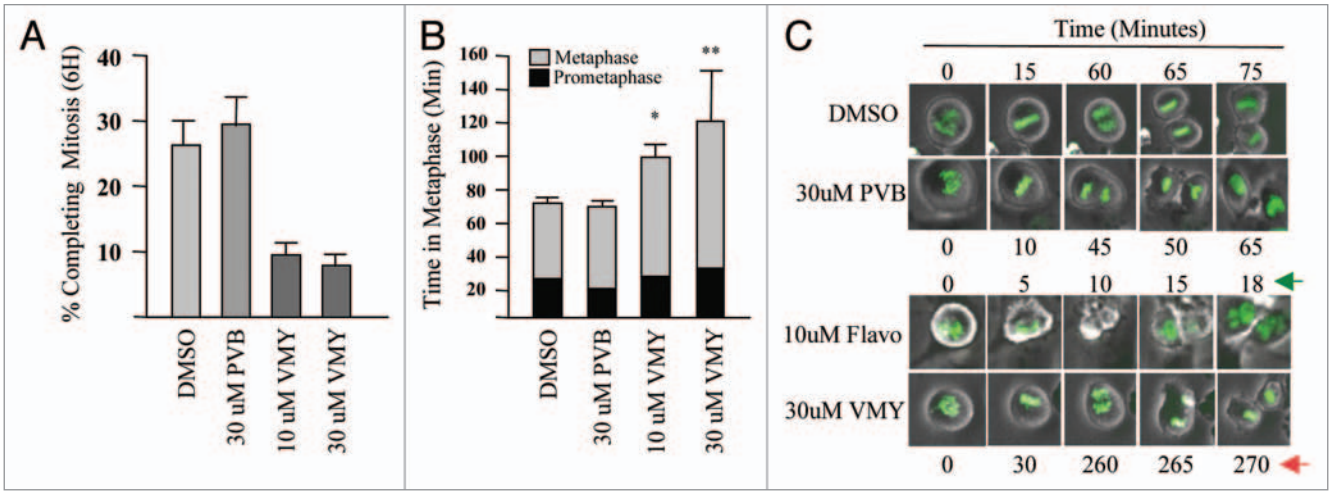


**Figure 3.** VMY-induced disruption of mitosis in DAOY cells. Live cell imaging was performed using stably transfected DAOY/GFP-H2B cells. (A) The percent of cells that successfully completed mitosis within 6 h following release from nocodazole block. (B) Metaphase transit time. (C) Examples of transit times of cells that successfully progressed through metaphase. Data are average percent change (+ SD, n > 250 cells, two separate experiments). Arrows, significant changes in mitotic progression in VMY vs. Flavo (flavopiridol) treated cells.

visualization of chromosomal activity in living cells using time lapsed video microscopy. DAOY/H2B-GFP cells were synchronized with nocodazole for 18 h, resulting in more than 90% of the cells arresting in $G_2$ (not shown). Nocodazole was removed from the cells followed by fresh culture media containing either DMSO, PVB, flavopiridol or VMY. The time of progression through mitosis was quantified by live cell imaging using a Nikon Eclipse TE300 video microscope. By 6 h, 26% of control, and 28% of the PVB-treated DAOY/H2B-GFP cells underwent an orderly progression from prophase through metaphase into telophase (**Fig. 3A and C**). Treatment with flavopiridol resulted in a significant acceleration of mitotic progression (**Fig. 3C**). This acceleration, or "mitotic slippage," is frequently seen with CDK inhibitors such as purvalanol, roscovitine or flavopiridol,[16] and is the result the inhibition of cyclinB/CDK1 activity during mitosis.[17] Conversely, treatment with VMY significantly reduced the number of cells completing mitosis within 6 h to less than 10% at 30 uM (**Fig. 3A**), and significantly prolonged metaphase vs. PVB or vehicle (**Fig. 3B and C**). Stage-specific analyses of the mitotic transit times established that while treatment with 30 uM PVB resulted in a slight acceleration in the prophase to metaphase progression (**Fig. 4A**), treatment with VMY significantly delayed both the prophase to metaphase and metaphase to anaphase transitions (**Fig. 4A and B**). Similar results were seen in D556 cells, where VMY significantly delayed mitotic progression (**Fig. 5A and B**) while flavopiridol significantly shortened time in mitosis (**Fig. 5A and B**), which is again consistent with its ability to induce mitotic slippage.

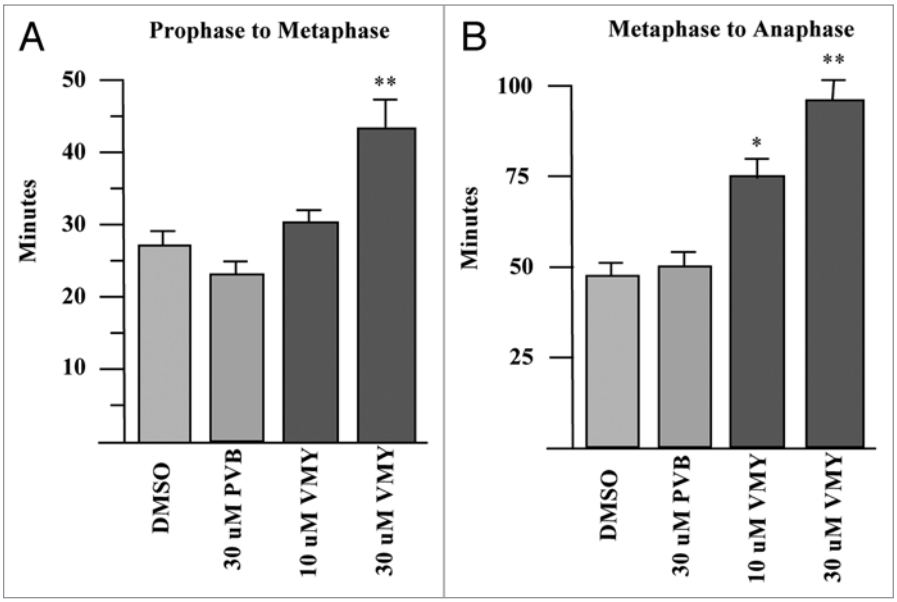


**Figure 4.** VMY delays progression through mitosis. DAOY/GFP-H2B cells were released from nocodazole block and followed by live-cell video microscopy. Time of progression from (A) prophase to metaphase and (B) metaphase to anaphase. *p ≤ 0.05, **p ≤ 0.01.

**VMY treatment disrupts centrosome polarity and induces mislocalization of chromosomes.** The Aurora-family of kinases is comprised of three genes *(aurka, aurkb* and *aurkc*) and Aurora Kinase A localizes to the centrosomes and spindle poles and regulates spindle assembly and centrosome maturation.[18] Aurora Kinase B acts in part to correct for misaligned chromosomes during mitosis,[19] and histone H3 that has been phosphorylated on serine 10 (p-HH3) by Aurora Kinase B is a marker of mitotic activity. The Wee1 kinase is a spindle pole associated protein during the $G_2$/M transition. Wee1 functions to regulate progression from $G_2$ into mitosis by inhibiting the activity of the cyclin

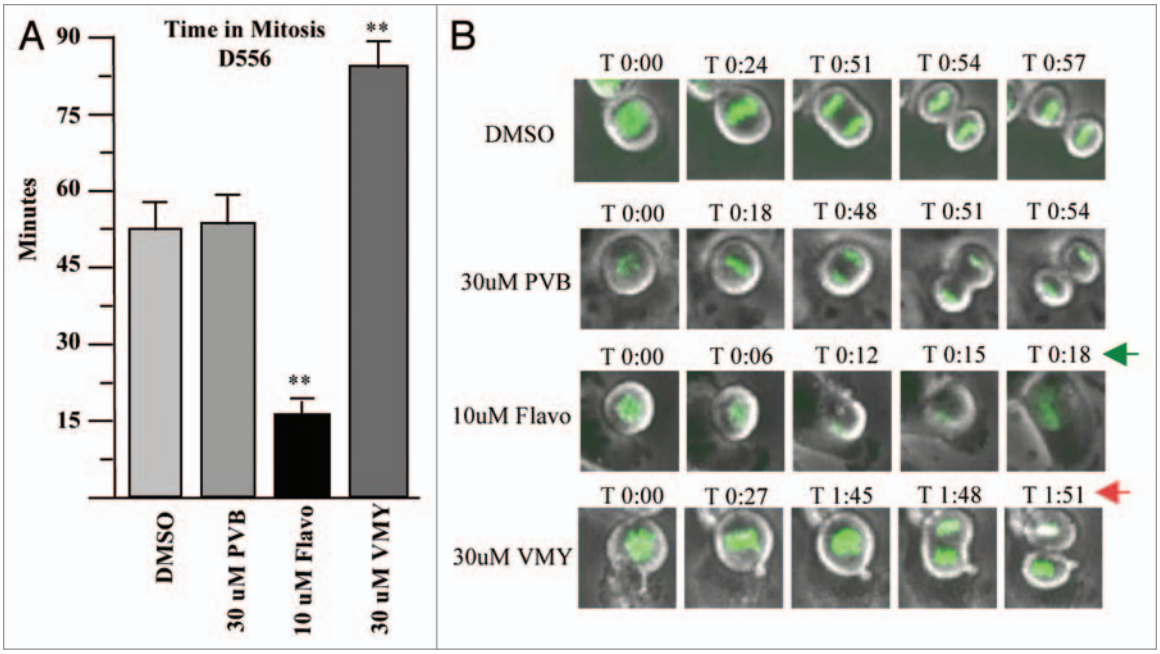


**Figure 5.** Effects of VMY and flavopiridol on Mitosis in D556 cells. Stable GFP-H2B/D556 cells were treated with nocodazole for 18 h. The nocodazole was removed and the cells were treated with the compounds as shown and followed by live cell imaging. (A) Average, n = four experiments. (B) Representative live cell images. **p < 0.01. Arrows, significant changes in mitotic progression in VMY vs. Flavo (flavopiridol) treated cells.

B/CDK1 holoenzyme complex via phosphorylation of CDK1 on tyrosines 14 and 15.

Based on our observations that VMY delayed the progression through mitosis, and to begin to understand the effect that VMY was having on the mitotic apparatus, randomly-cycling control and inhibitor-treated DAOY cells where probed with anti-Aurora A and p-HH3 antibodies and were counterstained with both phalloidin for F-actin and DAPI for chromatin.

In control cells, Aurora Kinase A immunofluorescence was centrally located within the chromatin during prometaphase, and was associated with the polar centrosome structures as the cells progressed into metaphase (**Fig. 6A**, *PM* and *M* respectively), consistent with its normal mitotic localization. The signal for p-HH3 localized to the end of the condensed chromosomes as expected (**Fig. 6A**). In contrast, within 1 h of treatment with VMY, mitotic abnormalities were evident, with cells exhibiting a disorganized alignment of the chromosomes (**Fig. 6B**, *PM* and *A*). In addition, while Aurora Kinase A staining remained localized to the centrosome, treatment with VMY resulted in a mislocalization of p-HH3 during all stages of mitosis (**Fig. 6B**). In those cells that were able to progress through metaphase, abnormalities such as lagging chromosomes persisted (**Fig. 6B**, *A* and *T*).

Control cells stained with Aurora Kinase A and phosphoserine 53-WEE1 andibodies, DAPI and phalloidin exhibited colocalized Aurora kinase A and Wee1 within the centrosome (**Fig. 6C**). While centrosome polarity was disrupted during prometaphase and metaphase, treatment with VMY did not appear to disrupt Aurora kinase A and Wee1 colocalization, despite its effect on chromosomal organization and migration. Protein gel blotting performed on extracts from DAOY cells treated for 1 h with PVB, VMY or flavopiridol following release from an 18 h nocodazole block established that the abundance tyrosine-15-phosphorylated CDK1 was not significantly affected by treatment with PVB, VMY or flavopiridol (**Fig. S2**), suggesting that VMY was not inhibiting Wee1 kinase activity during that time period. Aurora Kinase A levels were not affected by VMY or PVB, but were decreased following 1 h treatment with flavopiridol (**Fig. S3**), perhaps due to the mitotic slippage induced by flavopiridol.

## Discussion

Like many cancers, the etiology of MB is diverse, and a complex array of developmental and cell cycle regulatory genes, proteins and signaling pathways have been found to be compromised in both clinical samples[4-6] and in animal models.[20,21] Regardless of the underlying genetic or molecular abnormality, these tumors are highly proliferative, and advances in clinical treatment will require developing therapies that effectively target critical components of the cell proliferation machinery. This approach is underscored by the observation that Hh signaling pathway inhibitors such as GDC-0449, while initially successful in treating adult MB, induced or supported activating somatic mutations that ultimately resulted in disease recurrence.[22] We[9] and others[23] have recently explored the possibility that inhibiting the transcription factor, Gli, with arsenic trioxide may effectively block MB proliferation in culture and in mouse models of MB.

In the present report, we describe the effects of a new CDK-inhibitor developed by our group on cell proliferation and apoptosis in human medulloblastoma cell lines. Collectively the data

presented indicate that VMY induced cell cycle arrest and induced apoptosis at concentrations that were significantly lower than its parent compound, PVB, consistent with our previous studies.[13,14] VMY was also capable of significantly inhibiting CDK1 kinase activity but while flavopiridol induced mitotic slippage, VMY significantly delayed completion of prometaphase and metaphase, in part through interfering with chromosomal organization, thereby disrupting the orderly progression through mitosis. We conclude that a component of VMY's antiproliferative activity is the result of an induction of induction of apoptosis during mitosis, a process that has been referred to as mitotic catastrophe.[24]

The cyclin B/CDK1 complex is a key regulator of cell division. Orderly progression from $G_2$ to M requires a phosphorylation-dependent inhibition of CDK1 on Thr14 and Tyr 15 by Wee1/MYT1 in $G_2$, enabling the proper timing of entry into mitosis. As cells progress into M, the cyclin B/CDK1 complex is activated via dephosphorylation of the CDK1 Thr14 and Tyr 15 residues by the Cdc25C phosphatase. For cells to continue to progress through metaphase and complete cell division, cyclin B/CDK1 activity has to again be suppressed, occurring through degradation of cyclin B via the APC/C complex and the ubiquitin/proteosome pathway.[25] Because the suppression of cyclin B/CDK1 activity during mitosis is prerequisite for M-phase progression, CDK1 inhibitors such as PVB and flavopiridol have been found to induce mitotic slippage and accelerate mitosis and cytokinesis. For example, experiments performed in mitotically inhibited HeLa cells established that inhibition of CDK1 with PVB resulted in an accelerated mitotic exit and premature cytokinesis.[26] Mitotic slippage was also seen in taxane-inhibited cells treated with flavopiridol.[27] It is generally believed that mitotic slippage inhibits M-phase apoptosis but can result in $G_1$ arrest and apoptosis due to anueploidy.[28] We found that while treatment of MB cells with flavopiridol, and to a much lesser extent purvalanol B, resulted mitotic slippage, VMY not only failed to affect mitotic slippage, but induced a prolonged prometaphase/metaphase arrest which was due, at least in part, to a loss of normal chromosomal localization.

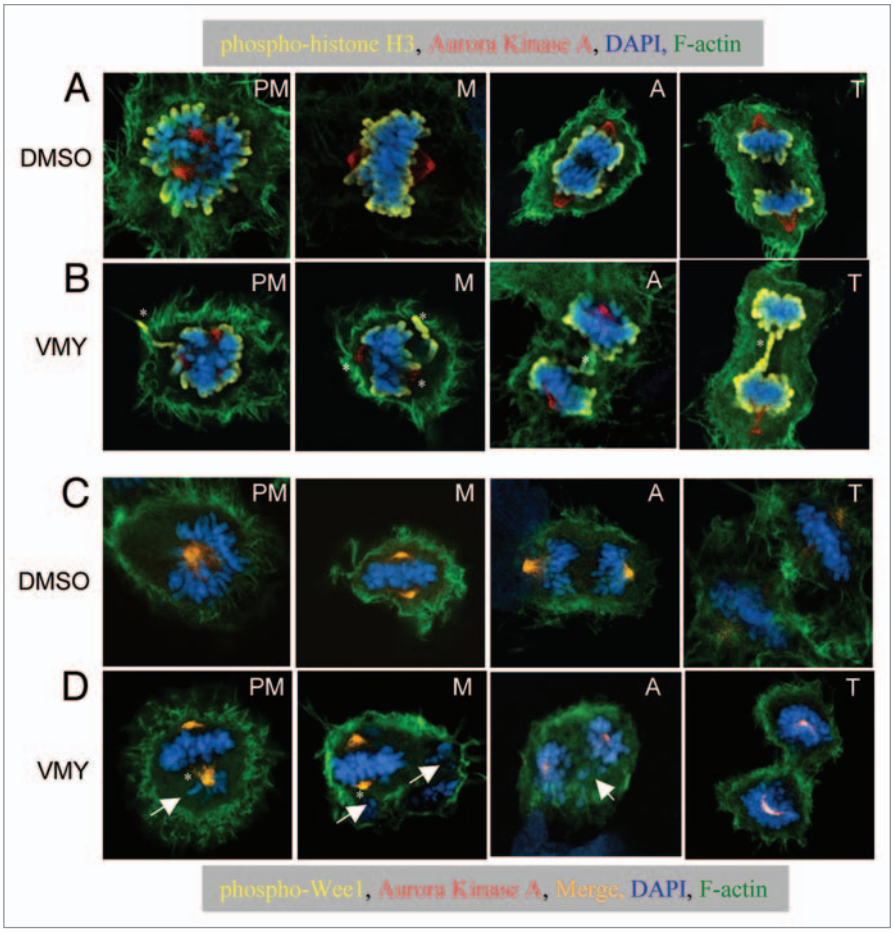


**Figure 6.** Merged fluorescent imaging of DAOY cells. Cells were treated DMSO or VMY (30 um) for 1 h. (A and B) Cells were stained with phospho-histone H3 (yellow) and Aurora Kinase A antibodies (red) as well as with DAPI (blue) and phalloidin for F-actin (green). (C and D) Cells were stained with phospho-Wee1 (yellow) and Aurora Kinase A antibodies (red) as well as with DAPI (blue) and phalloidin for F-actin (green). The Wee1/Aurora A merge is in orange. PM, prometaphase; M, metaphase; A, anaphase; T, telophase. Arrows, trailing or misaligned chromosomes, *, mislocalized Wee1, Aurora Kinase A or phospho-histone H3.

VMY, like roscovitine and flavopiridol, can inhibit the CDK7/CAK and CDK9/Cyclin T1 kinases in vitro[14] which affect transcription via a phosphorylation-dependent regulation of the c-terminal domain of RNA polymerase II. The *cyclin D1* and *p21$^{CIP1/WAF1}$* genes are known targets. We have shown that protein abundance of p21$^{CIP1/WAF1}$ was significantly decreased by VMY (**Fig. 2**) and as well as by flavopiridol (**Fig. S1**). Cyclin D1 levels also were reduced (Ringer L, Albanese C, unpublished) however no change in the $G_1$ fraction of cells was observed (**Fig. 1**). The functional consequences of the reduction of these proteins and whether regulation occurs at the level of RNA polymerase II is not known at this time. Hyperphosphorylated p21$^{CIP1/WAF1}$ has been shown to activate the CDK1/Cyclin B complex during the $G_2$/M transition[29] and a loss of p21$^{CIP1/WAF1}$ may delay mitosis. However, since both VMY and flavopiridol cause a similar reduction in protein levels, the loss of p21$^{CIP1/WAF1}$ cannot explain the differential effects on mitotoic progression seen between the two compounds.

While VMY does not appear to promote a complete disorganization of the centrosome, alterations were clearly evident, including compromised polarity. Defects in centrosome structure or function can have profound influences on mitosis, and cells that undergo a prolonged mitotic arrest become susceptible to mitotic apoptosis, which occurs when a cell is unable to fulfill its spindle checkpoint function. Commonly used chemotherapeutic agents such as the taxanes and vincristine, as well as inhibitors of key

mitosis-related kinases, such as the Aurora or Polo-like kinases, induce mitotic apoptosis through disruption of the mitotic spindle (reviewed in ref. 30), highlighting the mitotic checkpoint as a target for intervention. While the mechanisms by which VMY interfered with both chromosome alignment during metaphase and their migration during anaphase and telophase are not yet known, the rapid mitotic disruption observed with VMY clearly differentiates this compound from its parent, PVB, as well as from flavopiridol. These non-classical spindle-disrupting capabilities of VMY in combination with its classical CDK-inhibitory activity suggest that VMY represents a new sub-class of small molecule CDK inhibitor. Our data warrant further investigations into the anti-mitotic mechanisms of action of VMY both in vitro and in preclinical MB models.[9]

## Materials and Methods

**Cell lines and cell culture.** The human medulloblastoma cell lines, DAOY and D556 were maintained in RPMI, with 10% FCS, 0.1 mM non-essential amino acids, 100 U/ml Penicillin-Streptomycin and 1 mM sodium pyruvate at 37°C in 5% $CO_2$ as previously described in references 9 and 10. The PI3K inhibitor LY294002 (Sigma), the parent CDK inhibitor purvalanol B (Sigma), flavopiridol (Sigma), or VMY-1-103,[13,14] were added to the culture medium for up to 18 h. DMSO was used as vehicle control. The $ED_{50}$s were calculated using Prism (GraphPad). To label chromatin, DAOY cells were stably transfected with pEGFP-N1-Histone2B-GFP plasmid (a gift from Susette Mueller). Briefly, a 10 cm dish of DAOY cells was transfected with 10 μg of GFP/H2B in media containing 10% FBS using fugene 6 (Roche). After 48 h, the cells were split into three 10 cm dishes and 400 μg/ml G418 (Invitrogen) was added. Positive colonies were identified by fluorescence microscopy and six individual clones were selected. The cells were treated with VMY followed by cell cycle analyses and comparisons were made to untransfected cells to ensure there were no changes in the cells sensitivity to the drug.

**Flow-cytometry.** The medulloblastoma cells were collected by trypsinization, fixed in 10% ethanol and resuspended in PBS containing 20 μg/ml propidium iodide (PI) and 5 U RNase A. DNA content was measured using a FACStar Plus dual laser FACSort system (Becton-Dickinson) as previously described in references 13, 31 and 32.

**Immunoblotting.** Protein extracts were separated on 4–20% Tris-glycine gels and electro-blotted onto nitrocellulose.[13,33] Protein levels were assessed using antibodies against cyclin B1, cleaved caspase-3 and PARP and $p21^{CIP1}$, as previously described in reference 13. Anti-β-actin (Cell Signaling, 4967) was used as loading control as previously described in reference 13.

**Cell viability and growth.** Following inhibitor treatment, cell viability was determined by trypan blue exclusion. For apoptosis assays, Proteome Profiler human apoptosis arrays (R&D Systems) were performed as previously described in reference 13 as per the manufacturer's protocol. Briefly, nitrocellulose membranes (spotted with 35 antibodies, in duplicate) were blocked with array buffer (supplied by the manufacturer) for 1 h at room temperature, the membranes were washed and incubated with 500 μg of protein overnight at 4°C. A biotinylated primary antibody (supplied by the manufacturer) was added for 1 h, followed by a 30 min incubation with Streptavidin-HRP, and finally with an ECL reagent (1:3,000; Pierce). Array data were developed on X-ray film and spot areas and intensities were analyzed using ImageJ (NIH) as previously described in reference 13.

**Fluorescence imaging.** Cells were seeded on glass coverslips and treated with DMSO or inhibitors for 1 h. Cells were washed with PBS and fixed in 10% formalin for 10 min. Cells were then washed three times with PBS, permeabilized with 0.1% Triton X-100, and washed an additional three times with PBS. Cells were then incubated with the following primary antibodies: p-Wee1 (Ser 53, 1:50, Santa Cruz), Aurora A (1:100, BD Biosciences), and p-Histone H3 (S10, 1:200, Cell Signaling) for 1 hr at room temperature. Slides were then washed with PBS an additional three times and stained with the following secondary antibodies for 30 min at room temperature: Cy5 donkey anti-rabbit (1:200, Invitrogen) and Texas Red donkey anti-mouse (1:200). Slides were then counterstained with DAPI and 488-Phalloidin (1:200, Invitrogen) for 5 min. The coverslips were mounted onto glass slides with Tris-buffered fluoro-gel (Electron Microscopy Sciences). Confocal microscopy was performed on an Olympus Fluoview-FV300 Laser Scanning Confocal System (100x lens, oil immersion).

**Live cell imaging.** Automated time-lapse microscopy was performed on a Nikon Eclipse TE-300 Inverted Spinning Disc Confocal Microscope System. Cells were maintained in a microscope stage incubator at 37°C in a humidified atmosphere of 5% $CO_2$ throughout the experiment. Confocal microscopy was performed using a 40x lens. Images and time-lapse videos were obtained using Velocity (v 5.3.1) image acquisition and analysis software by Improvision. To image time in mitosis, stable GFP-H2B DAOY cells were seeded in a 12-well glass-bottom dish (MatTek) and were synchronized in the $G_2$ phase of the cell cycle with 20 ng/ml nocodazole for 12 h. Ten to twenty cells were selected in each well using the Velocity software, and imaged in the presence of nocodazole. Media containing nocodazole was then removed from the dish and the cells were washed three times with PBS. Cell culture media was replaced containing DMSO, Purvalanol B, Flavopiridol or VMY-1-103. Cells were immediately imaged every 2 min for 12 h. Ten Z-stack sections were taken images were taken per cell (3 uM spacing between slices) with a GFP (488 nm) laser. One bright-field image was taken in the center of each cell as a reference point. Mitotic cells were quantified and manually analyzed for time in mitosis.

**Cdk1 kinase assays.** Ten centimeter dishes of 80% confluent DAOY cells were placed on ice for 10 min and scraped into the culture medium. The cells were collected by centrifugation for 5 min at 500 g, washed with 10 ml PBS containing 1 mM $MgCl_2$ and resuspended in 1.0 ml kinase assay buffer (25 mM β-glycerophosphate, 25 mM (4-(2-hydroxyethyl)-1-piperazineethanesulfonic acid)-KOH (pH 7.4), 10 mM $MgCl_2$, 5 mM ethylene glycol tetraacetic acid, 1 mM dithiothreitol,

0.5 mM phenylmethylsulfonyl fluoride, 0.1 mM $Na_3VO_4$, 1 μg/ml aprotinin, 1 μg/ml leupeptin, 1 μg/ml pepstatin) at 4°C. Lysates were prepared using ultrasonic disruption at 4°C and immediately assayed for kinase activity. For each lysate, parallel assays were performed for 12 min at 33°C in the presence and absence of 0.1 mM CSH103 cdk1 substrate peptide (ADA QHA TPP KKK RKV ED; Enzo Life Sciences), and included (in a total volume of 100 μl) 10–20 μl lysate, 0.1 mM ATP and 0.1 mCi/ml γ-[$^{32}$P]ATP (7,000 Ci/mmol; MP Biomedicals). To determine levels of phosphorylation, 25 μl aliquots of assays were spotted on 2.3 cm P81 cellulose phosphate filters (Whatman) followed by five washes with 100 ml 1% (v/v) $H_3PO_4$ (≥5 min per wash). Washed filters were transferred to 20 ml glass vials for scintillation counting following addition of 10 ml BioSafe II scintillation cocktail (Research Products International). Counts were normalized for [$^{32}$P]ATP specific activity and lysate protein concentration; determined using the Bio-Rad protein assay with a bovine IgG standard.

### Disclosure of Potential Conflicts of Interest

A patent application has been filed by Georgetown University on the behalf of the inventors Venkata Yenugonda and Milton L. Brown that are listed as authors in this article.

### Acknowledgments

We thank the Flow Cytometry and the Microscopy and Imaging Shared Resources of the Georgetown Lombardi Comprehensive Cancer Center. We thank Susette Mueller for the EGFP Histone H2B expression vector and for her help and expertise related to live cell imaging. This work was supported by the Georgetown Drug Discovery Program and by P30 CA51008, R01CA129003 (C.A.), ABC2 (C.A. and T.M.).

### Note

Supplemental materials can be found at:
www.landesbioscience.com/journals/cbt/article/17682/.

### References

1. Hatten ME, Roussel MF. Development and cancer of the cerebellum. Trends Neurosci 2011; 34:134-42; PMID:21315459; DOI:10.1016/j.tins.2011.01.002.
2. Saury JM, Emanuelson I. Cognitive consequences of the treatment of medulloblastoma among children. Pediatr Neurol 2011; 44:21-30; PMID:21147383; DOI:10.1016/j.pediatrneurol.2010.07.004.
3. Roussel MF, Robinson G. Medulloblastoma: advances and challenges. F1000 Biol Rep 2011; 3:5; PMID:21655335; DOI:10.3410/B3-5.
4. Kool M, Koster J, Bunt J, Hasselt NE, Lakeman A, van Sluis P, et al. Integrated genomics identifies five medulloblastoma subtypes with distinct genetic profiles, pathway signatures and clinicopathological features. PLoS ONE 2008; 3:3088; PMID:18769486; DOI:10.1371/journal.pone.0003088.
5. Northcott PA, Korshunov A, Witt H, Hielscher T, Eberhart CG, Mack S, et al. Medulloblastoma Comprises Four Distinct Molecular Variants. J Clin Oncol 2011; 29:1408-14; PMID:20823417; DOI:10.1200/JCO.2009.27.4324.
6. Cho YJ, Tsherniak A, Tamayo P, Santagata S, Ligon A, Greulich H, et al. Integrative genomic analysis of medulloblastoma identifies a molecular subgroup that drives poor clinical outcome. J Clin Oncol 2011; 29:1424-30; PMID:21098324; DOI:10.1200/JCO.2010.28.5148.
7. Marino S. Medulloblastoma: developmental mechanisms out of control. Trends Mol Med 2005; 11:17-22; PMID:15649818; DOI:10.1016/j.molmed.2004.11.008.
8. Bar EE, Chaudhry A, Farah MH, Eberhart CG. Hedgehog signaling promotes medulloblastoma survival via Bc/II. Am J Pathol 2007; 170:347-55; PMID:17200206; DOI:10.2353/ajpath.2007.060066.
9. Beauchamp EM, Ringer L, Bulut G, Sajwan KP, Hall MD, Lee YC, et al. Arsenic trioxide inhibits human cancer cell growth and tumor development in mice by blocking Hedgehog/GLI pathway. J Clin Invest 2011; 121:148-60; PMID:21183792; DOI:10.1172/JCI42874.
10. Abouantoun TJ, Castellino RC, MacDonald TJ. Sunitinib induces PTEN expression and inhibits PDGFR signaling and migration of medulloblastoma cells. J Neurooncol 2011; 101:215-26; PMID:20524040; DOI:10.1007/s11060-010-0259-9.
11. Pestell RG, Albanese C, Reutens AT, Segall JE, Lee RJ, Arnold A. The cyclins and cyclin-dependent kinase inhibitors in hormonal regulation of proliferation and differentiation. Endocr Rev 1999; 20:501-34; PMID:10453356; DOI:10.1210/er.20.4.501.
12. Chang YT, Gray NS, Rosania GR, Sutherlin DP, Kwon S, Norman TC, et al. Synthesis and application of functionally diverse 2,6,9-trisubstituted purine libraries as CDK inhibitors. Chem Biol 1999; 6:361-75; PMID:10375538; DOI:10.1016/S1074-5521(99)80048-9.
13. Ringer L, Yenugonda VM, Ghosh A, Divito K, Trabosh V, Patel Y, et al. VMY-1-103, a dansylated analog of purvalanol B, induces caspase-3-dependent apoptosis in LNCaP prostate cancer cells. Cancer Biol Ther 2010; 10:320-5; PMID:20574155; DOI:10.4161/cbt.10.4.12208.
14. Yenugonda VM, Deb TB, Grindrod SC, Dakshanamurthy S, Yang Y, Paige M, et al. Fluorescent cyclin-dependent kinase inhibitors block the proliferation of human breast cancer cells. Bioorg Med Chem 2011; 19:2714-25; PMID:21440449; DOI:10.1016/j.bmc.2011.02.052.
15. Lindqvist A, Rodriguez-Bravo V, Medema RH. The decision to enter mitosis: feedback and redundancy in the mitotic entry network. J Cell Biol 2009; 185:193-202; PMID:19364923; DOI:10.1083/jcb.200812045.
16. Potapova TA, Sivakumar S, Flynn JN, Li R, Gorbsky GJ. Mitotic progression becomes irreversible in prometaphase and collapses when Wee1 and Cdc25 are inhibited. Mol Biol Cell 2011; 22:1191-206; PMID:21325631; DOI:10.1091/mbc.E10-07-0599.
17. Shapiro GI. Cyclin-dependent kinase pathways as targets for cancer treatment. J Clin Oncol 2006; 24:1770-83; PMID:16603719; DOI:10.1200/JCO.2005.03.7689.
18. Lens SM, Voest EE, Medema RH. Shared and separate functions of polo-like kinases and aurora kinases in cancer. Nat Rev Cancer 2010; 10:825-41; PMID:21102634; DOI:10.1038/nrc2964.
19. Lampson MA, Cheeseman IM. Sensing centromere tension: Aurora B and the regulation of kinetochore function. Trends Cell Biol 2011; 21:133-40; PMID:21106376; DOI:10.1016/j.tcb.2010.10.007.
20. Saab R, Rodriguez-Galindo C, Matmati K, Rehg JE, Baumer SH, Khoury JD, et al. p18$^{Inkdc}$ and p53 Act as tumor suppressors in cyclin D1-driven primitive neuroectodermal tumor. Cancer Res 2009; 69:440-8; PMID:19147556; DOI:10.1158/0008-5472.CAN-08-1892.
21. Ayrault O, Zindy F, Rehg J, Sherr CJ, Roussel MF. Two tumor suppressors, p27$^{Kip1}$ and patched-1, collaborate to prevent medulloblastoma. Mol Cancer Res 2009; 7:33-40; PMID:19147535; DOI:10.1158/1541-7786.MCR-08-0369.
22. Yauch RL, Dijkgraaf GJ, Alicke B, Januario T, Ahn CP, Holcomb T, et al. Smoothened mutation confers resistance to a Hedgehog pathway inhibitor in medulloblastoma. Science 2009; 326:572-4; PMID:19726788; DOI:10.1126/science.1179386.
23. Kim J, Lee JJ, Kim J, Gardner D, Beachy PA. Arsenic antagonizes the Hedgehog pathway by preventing ciliary accumulation and reducing stability of the Gli2 transcriptional effector. Proc Natl Acad Sci USA 2010; 107:13432-7; PMID:20624968; DOI:10.1073/pnas.1006822107.
24. Galluzzi L, Aaronson SA, Abrams J, Alnemri ES, Andrews DW, Baehrecke EH, et al. Guidelines for the use and interpretation of assays for monitoring cell death in higher eukaryotes. Cell Death Differ 2009; 16:1093-107; PMID:19373242; DOI:10.1038/cdd.2009.44.
25. Ma HT, Poon RY. How protein kinases co-ordinate mitosis in animal cells. Biochem J 2011; 435:17-31; PMID:21406064; DOI:10.1042/BJ20100284.
26. Niiya F, Xie X, Lee KS, Inoue H, Miki T. Inhibition of cyclin-dependent kinase 1 induces cytokinesis without chromosome segregation in an ECT2 and MgcRacGAP-dependent manner. J Biol Chem 2005; 280:36502-9; PMID:16118207; DOI:10.1074/jbc.M508007200.
27. Shapiro EM, Skrtic S, Sharer K, Hill JM, Dunbar CE, Koretsky AP. MRI detection of single particles for cellular imaging. Proc Natl Acad Sci USA 2004; 101:10901-6; PMID:15256592; DOI:10.1073/pnas.0403918101.
28. Blagosklonny MV. Mitotic arrest and cell fate: why and how mitotic inhibition of transcription drives mutually exclusive events. Cell Cycle 2007; 6:70-4; PMID:17245109; DOI:10.4161/cc.6.1.3682.
29. Dash BC, El-Deiry WS. Phosphorylation of p21 in $G_2$/M promotes cyclin B-Cdc2 kinase activity. Mol Cell Biol 2005; 25:3364-87; PMID:15798220; DOI:10.1128/MCB.25.8.3364-87.2005.
30. Vakifahmetoglu H, Olsson M, Zhivotovsky B. Death through a tragedy: mitotic catastrophe. Cell Death Differ 2008; 15:1153-62; PMID:18404154; DOI:10.1038/cdd.2008.47.
31. Albanese C, D'Amico M, Reutens AT, Fu M, Watanabe G, Lee RJ, et al. Activation of the *cyclin D1* gene by the E1A-associated protein p300 through AP-1 inhibits cellular apoptosis. J Biol Chem 1999; 274:34186-95; PMID:10567390; DOI:10.1074/jbc.274.48.34186.
32. Albanese C, Wu K, D'Amico M, Jarrett C, Joyce D, Hughes J, et al. IKKalpha Regulates Mitogenic Signaling through Transcriptional Induction of Cyclin D1 via Tcf. Mol Biol Cell 2003; 14:585-99; PMID:12589056; DOI:10.1091/mbc.02-06-0101.
33. Casimiro M, Rodriguez O, Pootrakul L, Aventian M, Lushina N, Cromelin C, et al. ErbB-2 induces the cyclin D1 gene in prostate epithelial cells in vitro and in vivo. Cancer Res 2007; 67:4364-72; PMID:17483350; DOI:10.1158/0008-5472.CAN-06-1898.